SECURITY INFORMATION

CONFIDENTIAL

NACA RM A53D06

3 1176 00005 9007

JUN 10 1953

NACA

RESEARCH MEMORANDUM

THE EFFECTS OF NACELLES AND OF EXTENDED SPLIT FLAPS ON THE LONGITUDINAL CHARACTERISTICS OF A WING-FUSELAGE-TAIL COMBINATION HAVING A WING WITH 40° OF SWEEPBACK AND AN ASPECT RATIO OF 10

By Bruce E. Tinling and Armando E. Lopez

Ames Aeronautical Laboratory
Moffett Field, Calif.

CLASSIFICATION CANCELLED

Authority NACA RM 36 9 5 Date 9/15/55

By [illegible] See [illegible]

CLASSIFIED DOCUMENT

This material contains information affecting the National Defense of the United States within the meaning of the espionage laws, Title 18, U.S.C., Secs. 793 and 794, the transmission or revelation of which in any manner to an unauthorized person is prohibited by law.

NATIONAL ADVISORY COMMITTEE
FOR AERONAUTICS

WASHINGTON

June 5, 1953

CONFIDENTIAL

NATIONAL ADVISORY COMMITTEE FOR AERONAUTICS

RESEARCH MEMORANDUM

THE EFFECTS OF NACELLES AND OF EXTENDED SPLIT FLAPS ON THE LONGITUDINAL CHARACTERISTICS OF A WING-FUSELAGE-TAIL COMBINATION HAVING A WING WITH 40° OF SWEEPBACK AND AN ASPECT RATIO OF 10

By Bruce E. Tinling and Armando E. Lopez

SUMMARY

An investigation has been conducted to evaluate the effects of nacelles and of extended split flaps on the longitudinal characteristics of a wing-fuselage-tail combination of a type believed suitable for long-range high-speed airplanes. The wing, which was cambered and twisted, had an aspect ratio of 10, a taper ratio of 0.4, and 40° of sweepback. The nacelles were at 25 and 50 percent of the semispan.

Wind-tunnel tests to study the effects of the nacelles were conducted at Mach numbers up to 0.90 at a wing Reynolds number of 2,000,000. Tests to evaluate the effects of flaps were conducted at a Reynolds number of 4,000,000 and a Mach number of 0.082.

The combined frontal area of the nacelles was equal to about 1-1/2 times that of the fuselage. The drag increment caused by the nacelles at low speed was equal to that caused by the fuselage but was much greater than the drag increment due to the fuselage at the higher Mach numbers. The nacelles caused reductions in both the wing and tail contributions to the static longitudinal stability.

The maximum lift coefficient for which the static longitudinal stability remained nearly constant and for which the model could be balanced was increased from about 1.2 at an angle of attack of 17° to about 1.5 at an angle of attack of 15° by deflecting the half-span extended split flaps 30°.

INTRODUCTION

The aerodynamic problems associated with long-range airplanes designed to fly at high subsonic speeds have been the subject of an investigation in the Ames 12-foot pressure wind tunnel. The longitudinal characteristics of a model of a wing-fuselage-tail combination believed to be suitable for this application have been presented in references 1 through 3. The present report is concerned with the effects of nacelles at Mach numbers up to 0.90 and of flaps at low speed on the longitudinal aerodynamic characteristics of this configuration. The tests to study the effects of nacelles were conducted at a Reynolds number of 2,000,000, and the tests to study the effects of flaps were conducted at a Reynolds number of 4,000,000.

NOTATION

Symbols and Parameters

A — geometric aspect ratio, $\frac{b^2}{2S}$

a — mean-line designation, fraction of chord over which design load is uniform

$\frac{b}{2}$ — wing semispan perpendicular to the plane of symmetry

C_D — drag coefficient, $\frac{\text{drag}}{qS}$

C_{D_o} — profile drag coefficient, assuming elliptical span load distribution, $C_D - \frac{C_L^2}{\pi A}$

C_L — lift coefficient, $\frac{\text{lift}}{qS}$

C_m — pitching-moment coefficient about the quarter point of the mean aerodynamic chord, $\frac{\text{pitching moment}}{qS\bar{c}}$

(See fig. 1(a) for location of wing moment center with respect to the fuselage.)

c — local chord parallel to the plane of symmetry

[redacted]

c' local chord normal to the reference sweep line

$\bar{c}$ mean aerodynamic chord, $\frac{\int_0^{b/2} c^2 dy}{\int_0^{b/2} c\, dy}$

c_{l_i} design section lift coefficient

i_t incidence of the horizontal tail with respect to the wing-root chord

l_t tail length, distance between the quarter points of the mean aerodynamic chords of the wing and the horizontal tail

M free-stream Mach number

q free-stream dynamic pressure

R Reynolds number, based on the wing mean aerodynamic chord

S area of semispan wing, flaps off

t wing section maximum thickness

y lateral distance from the plane of symmetry

z vertical distance from the plane of the wing-root chord and leading edge to the horizontal-tail hinge axis

α angle of attack of the wing chord at the plane of symmetry (referred to herein as the wing-root chord)

δ flap angle, measured relative to the local chord in planes normal to the reference sweep line

γ nacelle inclination, the angle between the root chord and the projection of the thrust axis on the plane of symmetry, positive, nose up

ϵ effective average downwash angle

φ angle of local wing chord relative to the wing-root chord, positive for washin, measured in planes parallel to the plane of symmetry

[redacted]

$\frac{\partial C_m}{\partial i_t}$ tail effectiveness parameter, measured at a constant angle of attack

$\eta\left(\frac{q_t}{q}\right)$ tail efficiency factor (ratio of the lift-curve slope of the horizontal tail when mounted on the fuselage in the flow field of the wing to the lift-curve slope of the isolated horizontal tail)

Subscript

t horizontal tail

MODEL

The geometry of the model is shown in figures 1(a) through 1(e) and in table I. The selection of the geometric properties and the details of the construction of the wing, the fences, the all-movable horizontal tail, and the fuselage have been discussed in references 1 and 2.

The shape and size of the nacelles (fig. 1(c)), as well as their location with respect to the plane of the wing-root chord and leading edge, were governed to a considerable extent by considerations other than aerodynamic. These considerations included space requirements for electric motors and gear boxes for driving model propellers, and provisions for access and removal of these units without impairing the strength of the wing. Therefore, the aerodynamic qualities of the nacelles in regard to drag and interference effects have probably been compromised to some extent. The angles of inclination of the nacelles with respect to the wing were selected to reduce the propeller vibratory stresses as discussed in reference 4.

The extended split flaps consisted of 1/8-inch-thick aluminum plates attached to the trailing edge of the wing. (See fig. 1(e).) The flaps were supported by fixed brackets from the lower surface of the wing and had a chord equal to 20 percent of the wing chord, measured perpendicular to the reference sweep line. The flaps extended spanwise from the fuselage to the outer nacelle. The gaps between the flap and the wing trailing edge, nacelles, and fuselage were sealed.

A photograph of the model mounted in the wind tunnel is shown in figure 2. The turntable upon which the model was mounted is directly connected to the balance system.

[redacted]

CORRECTIONS TO DATA

The data have been corrected for constriction effects due to the presence of the tunnel walls, for tunnel-wall interference originating from lift on the wing, and for drag tares caused by aerodynamic forces on the exposed portion of the turntable upon which the model was mounted. The magnitudes of these corrections have been reported in references 2 and 4.

Measurements of the static pressure on the tunnel walls during the tests at high angles of attack at the higher Mach numbers indicated a local Mach number greater than 1.0. Data obtained under these conditions have been faired with dotted lines to indicate that the wind tunnel may have been partially choked.

RESULTS AND DISCUSSION

Effects of Nacelles - Tail Off

The longitudinal characteristics of the wing-fuselage-nacelle combination are presented in figure 3. Comparisons of these data with those for the wing-fuselage combination are presented in figures 4 through 7. In figures 3 and 5, the profile drag coefficient $C_D - C_L^2/\pi A$ has been presented instead of the total drag coefficient. This method of presentation permits the drag data to be plotted to a large scale commensurate with the accuracy of the data. To convert the profile drag to total drag, it is merely necessary to add the theoretical induced drag for an elliptical span load distribution $C_{D_i} = C_L^2/10\,\pi$ to the plotted value of profile drag coefficient.

The addition of nacelles to the wing increased the lift-curve slope by roughly 12 percent. (See fig. 6.) The effect of the nacelles on the variation of pitching moment with lift may be seen from figure 4. As would be anticipated, the nacelles were destabilizing. The reduction in longitudinal stability throughout the Mach number range, as indicated by the change in dC_m/dC_L for $C_L = 0.4$, is shown in figure 6.

The increase in drag and the reduction in maximum lift-drag ratio caused by the addition of the nacelles is shown in figures 5, 6, and 7. Drag data for most of the combinations of components of the model have also been included in figure 5. Inspection of these data shows that at low speeds, the drag increment due to the nacelles is approximately equal to that due to the fuselage. At the higher Mach numbers, the drag increment due to the nacelles was greater than that caused by the fuselage. It must be considered, however, that the combined frontal area of the

two nacelles was roughly 1-1/2 times that of the fuselage (see table I). If the incremental drag coefficients are based on frontal area, the incremental drag coefficient of the nacelles for moderate lift coefficients is less than that of the fuselage for Mach numbers less than 0.80.

The effects of the nacelles on the Mach number for drag divergence, defined as the Mach number at which $dC_D/dM = 0.10$, is shown in the following table:

C_L	Mach number for drag divergence	
	Wing-fuselage	Wing-fuselage-nacelles
0.2	Not attained	0.85
.3	0.89	.84
.4	.87	.83
.5	.83	.80
.6	.79	.76
.7	.73	.70

Effects of Tail Height

The results of a series of tests to evaluate the effects of a change of vertical location of the horizontal tail are presented in figure 8. At low speed (fig. 8(a)), an increase in the lift coefficient for balance was the only effect of raising the tail from the plane of the wing-root chord and leading edge to 0.15 b/2 above this plane. At higher Mach numbers (figs. 8(b) and 8(c)), the reduction in stability in the upper lift-coefficient range became more severe as the tail was raised. At a Mach number of 0.80 (fig. 8(b)) this reduction was sufficient to cause longitudinal instability at a lift coefficient of about 0.7 for tail heights above the wing-chord plane.

Effects of Nacelles - Tail On

On the basis of the data on the effects of tail height, the lowest tail position $z/(b/2) = 0$ was selected for a study of the effects of nacelles on the tail-on longitudinal characteristics at Mach numbers of 0.25, 0.80, and 0.90. Lift and pitching-moment data for several tail incidences with the tail in this position are presented in figure 9. The effective downwash angles were evaluated from these data by the

method of reference 5. These effective downwash angles are compared with those for the same configuration without nacelles (ref. 2) in figure 10.

Measurements of the pitching-moment-curve slopes from figure 4 for moderate lift coefficients indicate that at Mach numbers up to 0.80, the reduction in static margin caused by the nacelles (indicated by a more positive value of dC_m/dC_L) is greater with the tail on than with the tail off by a factor of about 2. This difference can be explained by examination of the effects of the nacelles on the factors which comprise the contribution of the horizontal tail to the pitching-moment-curve slope. This contribution, neglecting the increment in lift-curve slope due to the horizontal tail, is proportional to

$$\frac{(dC_L/d\alpha)_t}{(dC_L/d\alpha)_{\text{tail off}}} \left[\eta(q_t/q)\right] \left[1 - (d\epsilon/d\alpha)\right]$$

The variations of these factors with lift coefficient for Mach numbers of 0.25 and 0.80 are shown in figure 11. The values of the lift-curve slope of the isolated horizontal tail $(dC_L/d\alpha)_t$ were obtained from reference 2, and $\eta(q_t/q)$ was calculated by the same method as in reference 5. At a Mach number of 0.25 (fig. 11(a)), the reduction in the stability contribution of the horizontal tail caused by the nacelles for lift coefficients less than about 0.9 was a result of decreases in $\frac{(dC_L/d\alpha)_t}{(dC_L/d\alpha)_{\text{tail off}}}$ and $1 - (d\epsilon/d\alpha)$. The decrease in $\frac{(dC_L/d\alpha)_t}{(dC_L/d\alpha)_{\text{tail off}}}$ merely reflects the effect of the increase in lift-curve slope caused by the nacelles, since $(dC_L/d\alpha)_t$ is the lift-curve slope of the isolated horizontal tail. At a Mach number of 0.80 and lift coefficients less than about 0.6, the nacelles caused a small decrease in $\eta(q_t/q)$ in addition to decreases in the other factors. (See fig. 11(b)).

Effects of Flaps

The increase in maximum lift coefficient and the reduction in the angle of attack required to attain a given lift coefficient resulting from deflection of the half-span extended split flaps are shown in figure 12. A deflection of 60° of the flaps increased the maximum lift coefficient of the wing-fuselage combination from about 1.3 to 1.6. Deflection of the flaps caused little change in either the slope of the tail-off pitching-moment curves or the tail-off pitching-moment coefficient for lift coefficients greater than about 0.6. The lift-drag ratio

[redacted]

was improved by deflection of the flaps at lift coefficients greater than about 1.15 (see fig. 13).

Data obtained to study the effects of extended split flaps on the lift and pitching-moment coefficients with the horizontal tail at either $z/(b/2) = 0$ or $z/(b/2) = 0.10$ are presented in figures 14 and 15, respectively. A deflection of 30° of the flaps increased the maximum lift coefficient for which the model could be balanced and for which the static longitudinal stability remained nearly constant from about 1.2 at an angle of attack of 17° to 1.5 at an angle of attack of 15°. The increase in lift coefficient attributable to the flaps at a given landing attitude can be shown by comparing the lift coefficient for balance for an angle of attack of 12° with the flaps up with that for the same angle of attack with the flaps deflected 30°. At this angle of attack, the lift coefficient at which the model was balanced with the flaps up was 0.90. (See fig. 14(a) or 15(a).) With the flaps deflected 30° (fig. 14(b) or 15(b)), the lift coefficient for balance was about 1.35.

Comparison of figures 14(a) and 14(b) or 15(a) and 15(b) indicates that deflection of the flaps reduced the static margin by about 0.06 and caused a large nose-up pitching moment. The decrease in static margin was caused by an increase in the lift-curve slope of the wing (a consequence of the increased area with the flaps deflected) and by an increase in $d\epsilon/d\alpha$ (fig. 16), both of which decreased the stability contribution of the horizontal tail. Deflection of the flaps had no effect on the tail effectiveness parameter $\partial C_m/\partial i_t$ and, hence, no effect on the tail efficiency factor $\eta(q_t/q)$. The increase in downwash angle (fig. 16) caused the large nose-up pitching moment accompanying deflection of the flaps.

CONCLUDING REMARKS

The results of wind-tunnel tests to evaluate the effects of nacelles and of extended split flaps on the longitudinal characteristics of a wing-fuselage-tail combination having a wing with 40° of sweepback and an aspect ratio of 10 have been presented.

The results indicate that the nacelles, which had a combined frontal area equal to about 1-1/2 times that of the fuselage, caused a drag increment at low speeds which was approximately equal to that of the fuselage. At the higher Mach numbers, the drag increment caused by the nacelles was considerably greater than that caused by the fuselage. The nacelles reduced the static longitudinal stability of the wing-fuselage combination and also reduced the stability contribution of the horizontal tail.

[redacted]

The maximum lift coefficient for which the static longitudinal stability remained nearly constant and for which the model could be balanced was increased from about 1.2 to 1.5 by 30° deflection of the half-span extended split flaps. The corresponding angles of attack were about 17° with the flaps up and 15° with the flaps deflected.

Ames Aeronautical Laboratory
National Advisory Committee for Aeronautics
Moffett Field, Calif.

REFERENCES

1. Edwards, George G., Tinling, Bruce E., and Ackerman, Arthur C.: The Longitudinal Characteristics at Mach Numbers up to 0.92 of a Cambered and Twisted Wing Having 40° of Sweepback and an Aspect Ratio of 10. NACA RM A52F18, 1952.

2. Tinling, Bruce E.: The Longitudinal Characteristics at Mach Numbers up to 0.9 of a Wing-Fuselage-Tail Combination Having a Wing with 40° of Sweepback and an Aspect Ratio of 10. NACA RM A52I19, 1952.

3. Boltz, Frederick W., and Shibata, Harry H.: Pressure Distribution at Mach Numbers up to 0.90 on a Cambered and Twisted Wing Having 40° of Sweepback and an Aspect Ratio of 10, Including the Effects of Fences. NACA RM A52K20, 1953.

4. Lopez, Armando E., and Dickson, Jerald K.: The Effects of Compressibility on the Upwash at the Propeller Planes of a Four-Engine Tractor Airplane Configuration Having a Wing with 40° of Sweepback and an Aspect Ratio of 10. NACA RM A53A30a, 1953.

5. Johnson, Ben H., Jr., and Rollins, Francis W.: Investigation of a Thin Wing of Aspect Ratio 4 in the Ames 12-Foot Pressure Wind Tunnel. V - Static Longitudinal Stability and Control Throughout the Subsonic Speed Range of a Semispan Model of a Supersonic Airplane. NACA RM A9I01, 1949.

[redacted]

TABLE I.- GEOMETRIC PROPERTIES OF THE MODEL

Wing	
Reference sweep line: Locus of the quarter chords of sections inclined 40° to the plane of symmetry	
Aspect ratio	10.0
Taper ratio	0.4
Sweepback	40°
Twist (washout at tip)	5°
Reference sections (normal to reference sweep line)	
Root — NACA 0014, a=0.8 (modified)	$c_{l_i} = 0.4$
Tip — NACA 0011, a=0.8 (modified)	$c_{l_i} = 0.4$
Area (semispan model)	6.944 ft²
Mean aerodynamic chord	1.251 ft
Flaps (20 percent c' extending from trailing edge)	
Area	0.696 ft²
Incidence (measured in the plane of symmetry)	3°
Nacelles	
Frontal area (each)	0.208 ft²
Inclination,	
Inner	-6.5°
Outer	-7.0°
Horizontal Tail	
Reference sweep line: Locus of quarter chords of sections inclined 40° to the plane of symmetry	
Aspect ratio	4.5
Taper ratio	0.4
Sweepback	40°
Reference section	NACA 0010
Tail length, l_t	$3.25\bar{c}$
Area (semispan model)	1.387 ft²
Mean aerodynamic chord	0.833 ft
Tail volume, $l_t/c\ (S_t/S_w)$	0.65
Tail heights (measured from the intersection of the fuselage center line and the plane of the wing-root chord and leading edge) z/(b/2)	0, 0.05, 0.10, or 0.15

[redacted]

TABLE I.- GEOMETRIC PROPERTIES OF THE MODEL - Concluded

Fuselage

Fineness ratio	12.6
Frontal area (semispan model)	0.273 ft^2

Fuselage coordinates:

Distance from nose, in.	Radius, in.
0	0
1.27	1.04
2.54	1.57
5.08	2.35
10.16	3.36
20.31	4.44
30.47	4.90
39.44	5.00
50.00	5.00
60.00	5.00
70.00	5.00
76.00	4.96
82.00	4.83
88.00	4.61
94.00	4.27
100.00	3.77
106.00	3.03
126.00	0

NACA

[redacted]

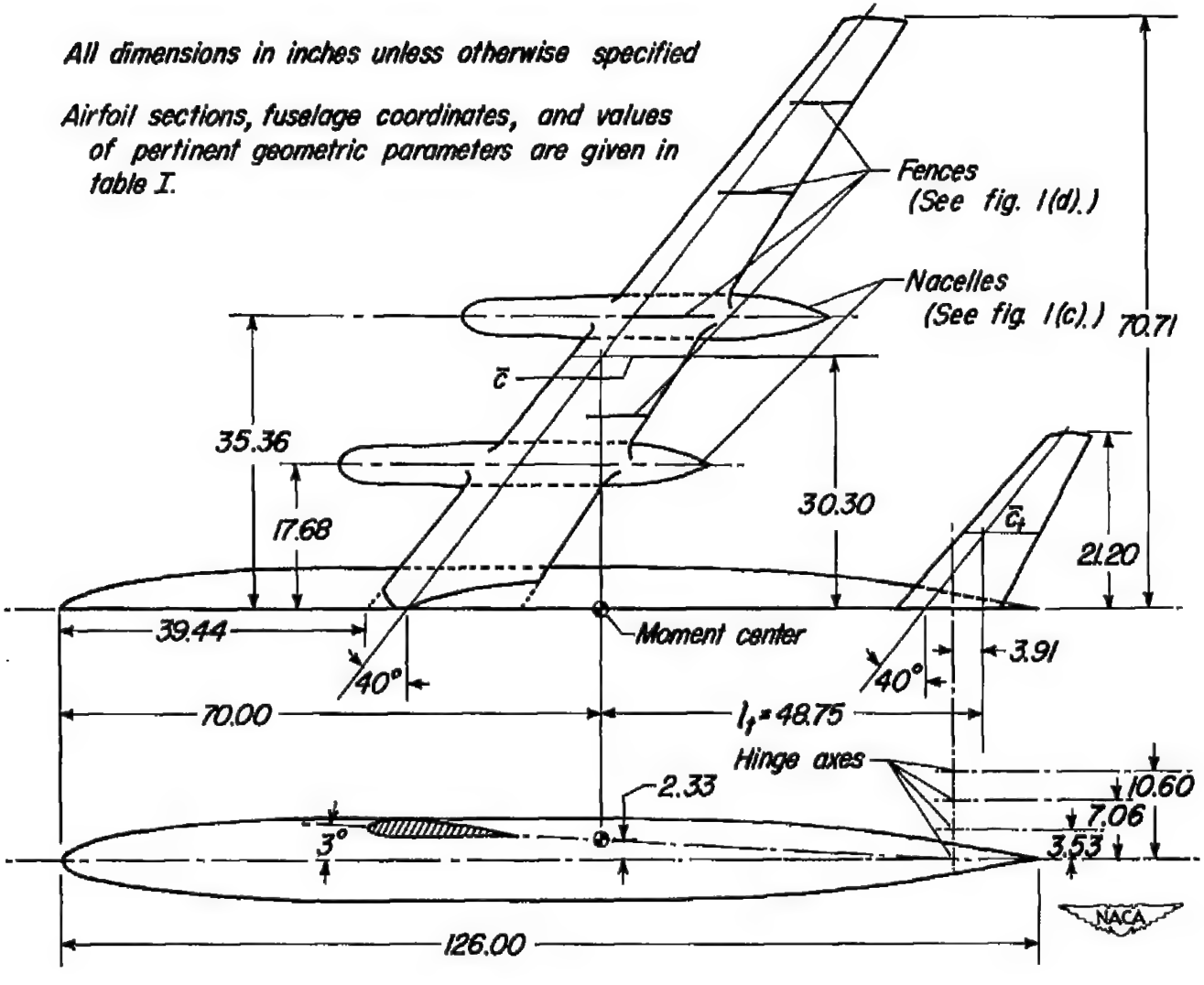

(a) Dimensions.

Figure 1.- Geometry of the model.

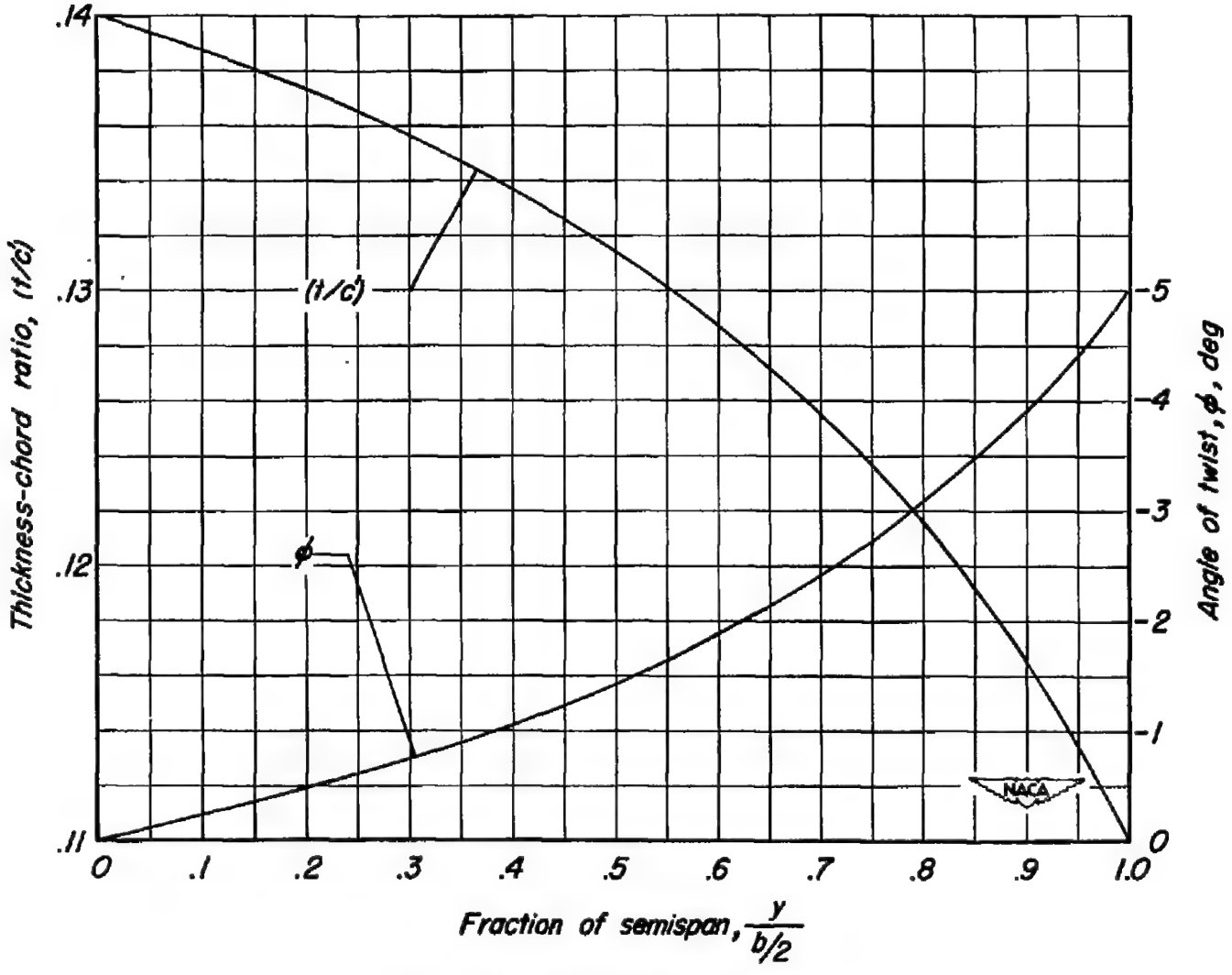

(b) Wing twist and thickness-chord ratio.

Figure 1.- Continued.

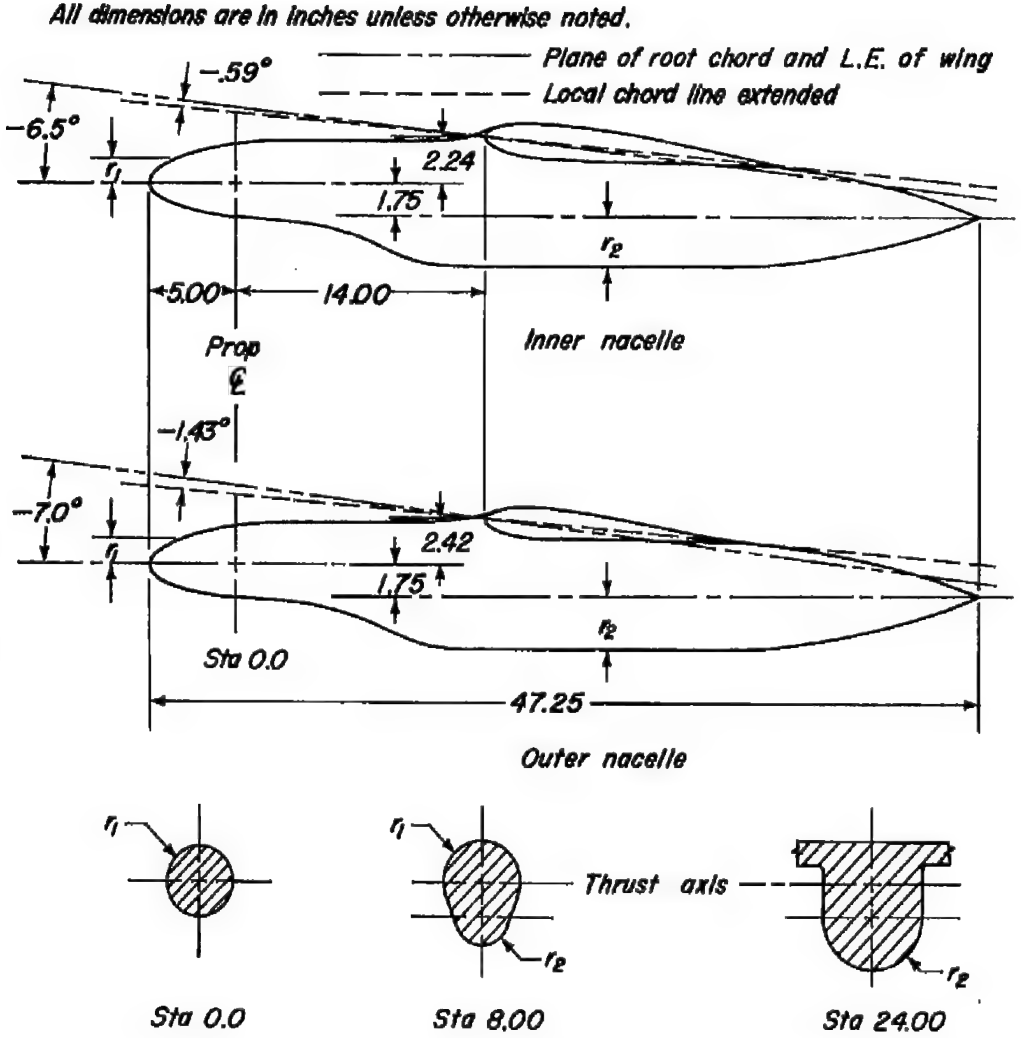

Nacelle coordinates

Sta	r_1	Sta	r_2
-5.00	0	2.00	0.350
-4.79	.385	3.00	.419
-4.58	.567	4.00	.616
-4.25	.788	5.00	.919
-3.95	.951	6.00	1.290
-3.25	1.242	7.00	1.685
-2.55	1.472	8.00	2.056
-1.80	1.670	9.00	2.359
- .80	1.871	10.00	2.556
0	1.985	11.00	2.625
2.00	2.100	30.50	2.625
12.00	2.100	32.50	2.450
		34.50	2.220
		36.50	1.825
		38.50	1.270
		40.50	.675
		41.50	.275
		42.25	0

NACA

A: .15

(c) Dimensions of nacelles.

Figure 1.- Continued.

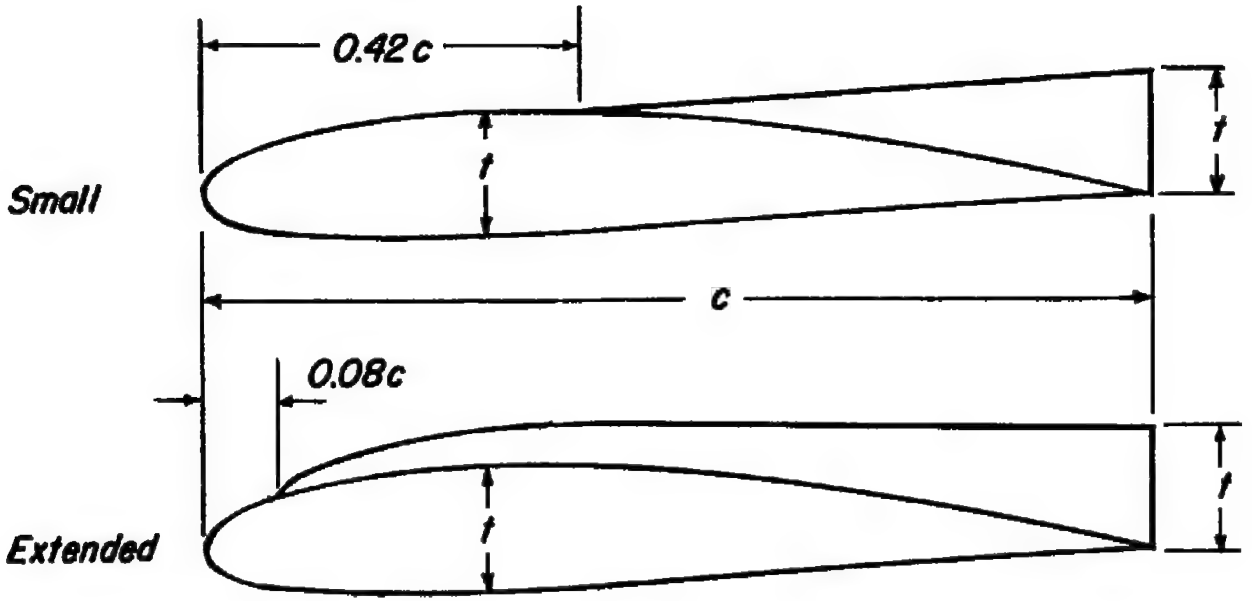

Type and location
Small at $\frac{y}{b/2} = 0.33$
Extended at $\frac{y}{b/2} = 0.50, 0.70,$ and 0.85

(d) Fence details.

Figure 1.- Continued.

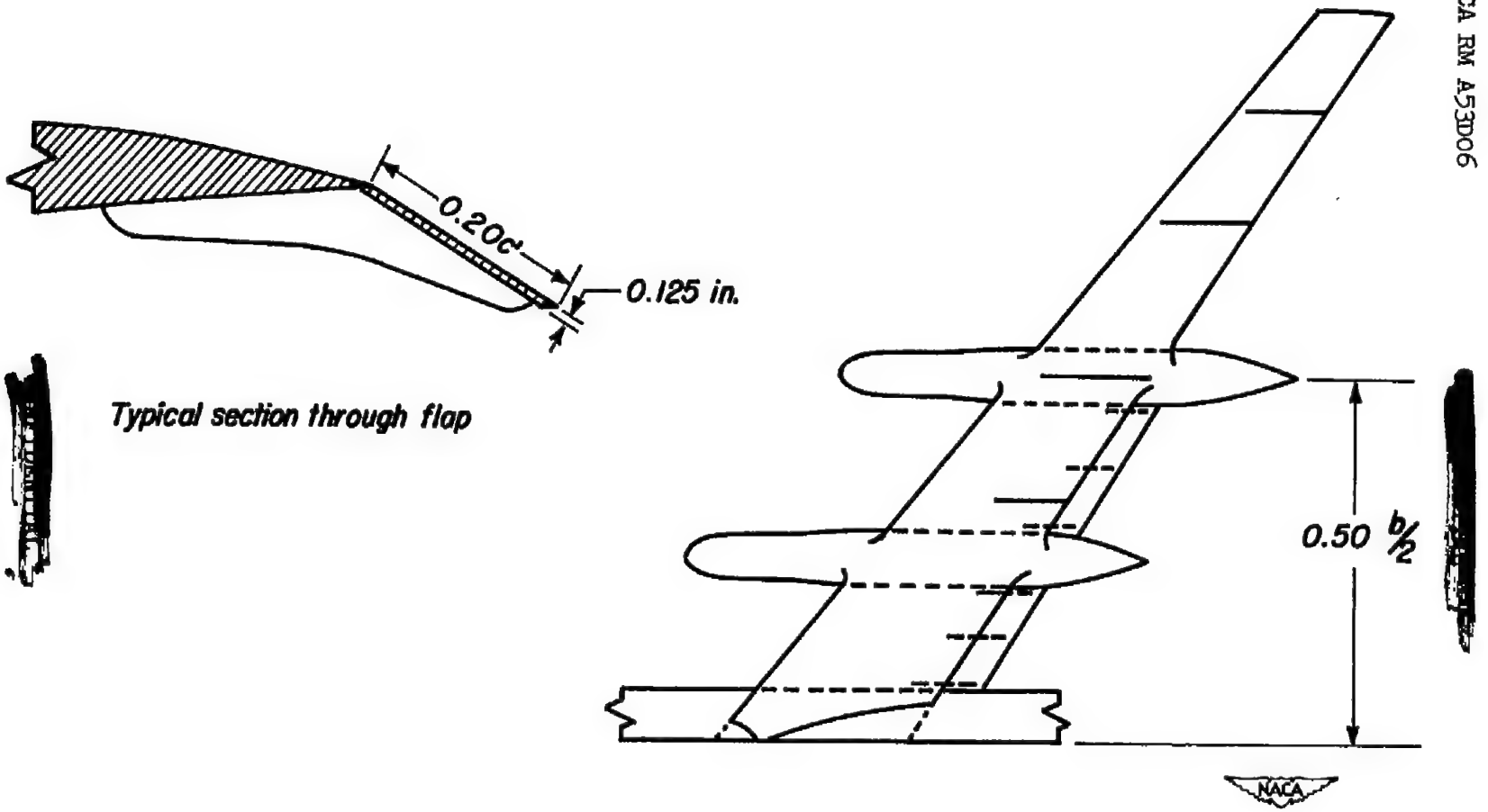

(e) Flap details.

Figure 1.- Concluded.

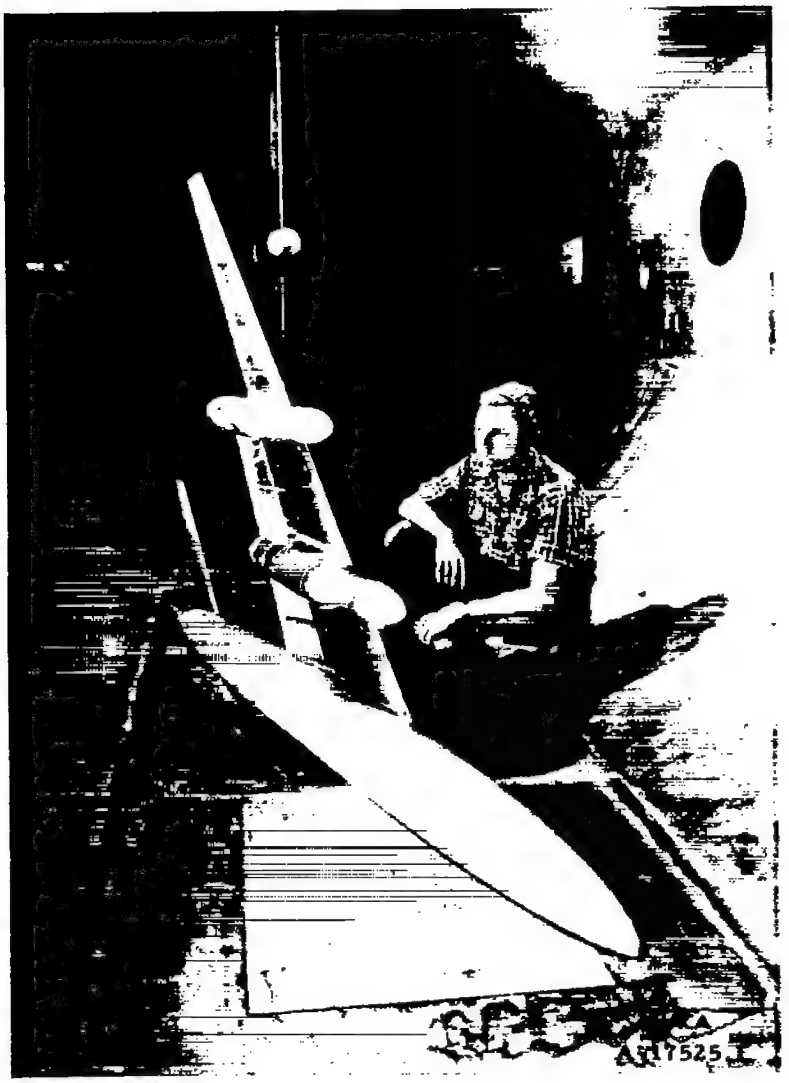

Figure 2.- Model mounted in the wind tunnel.

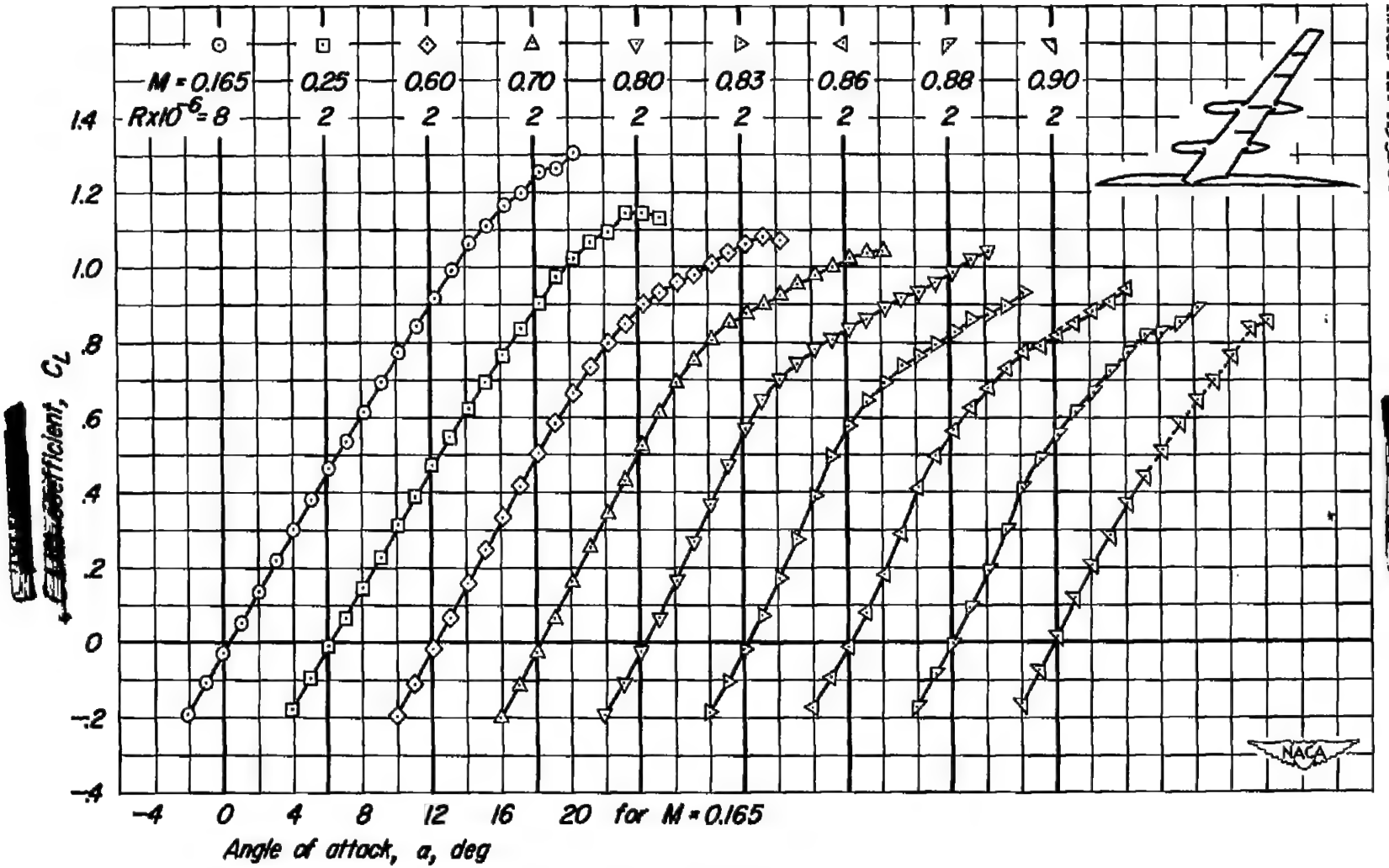

(a) C_L vs α

Figure 3.- The lift, drag, and pitching-moment coefficients of the wing-fuselage-nacelle combination.

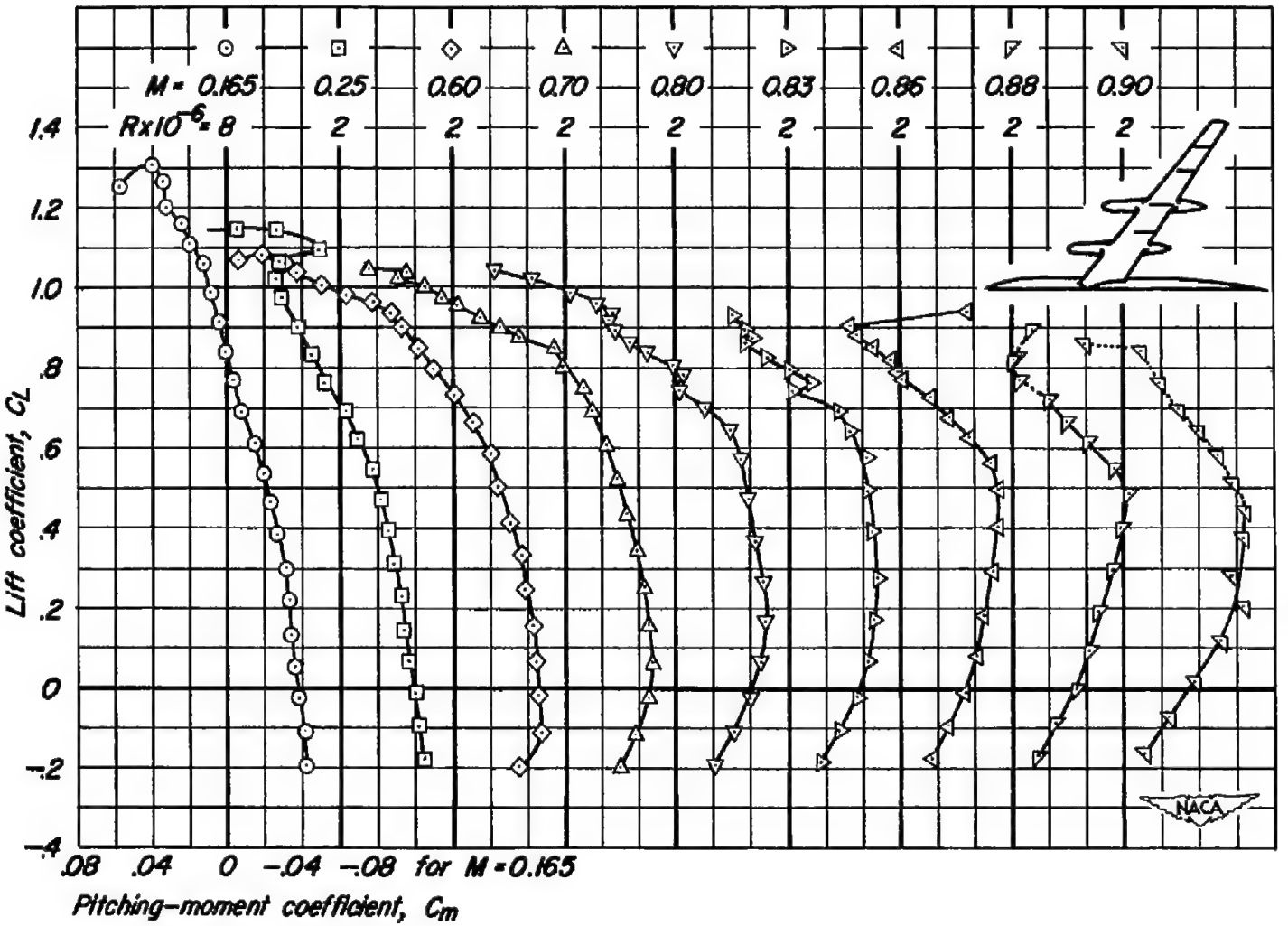

(b) C_M vs C_L

Figure 3.- Continued.

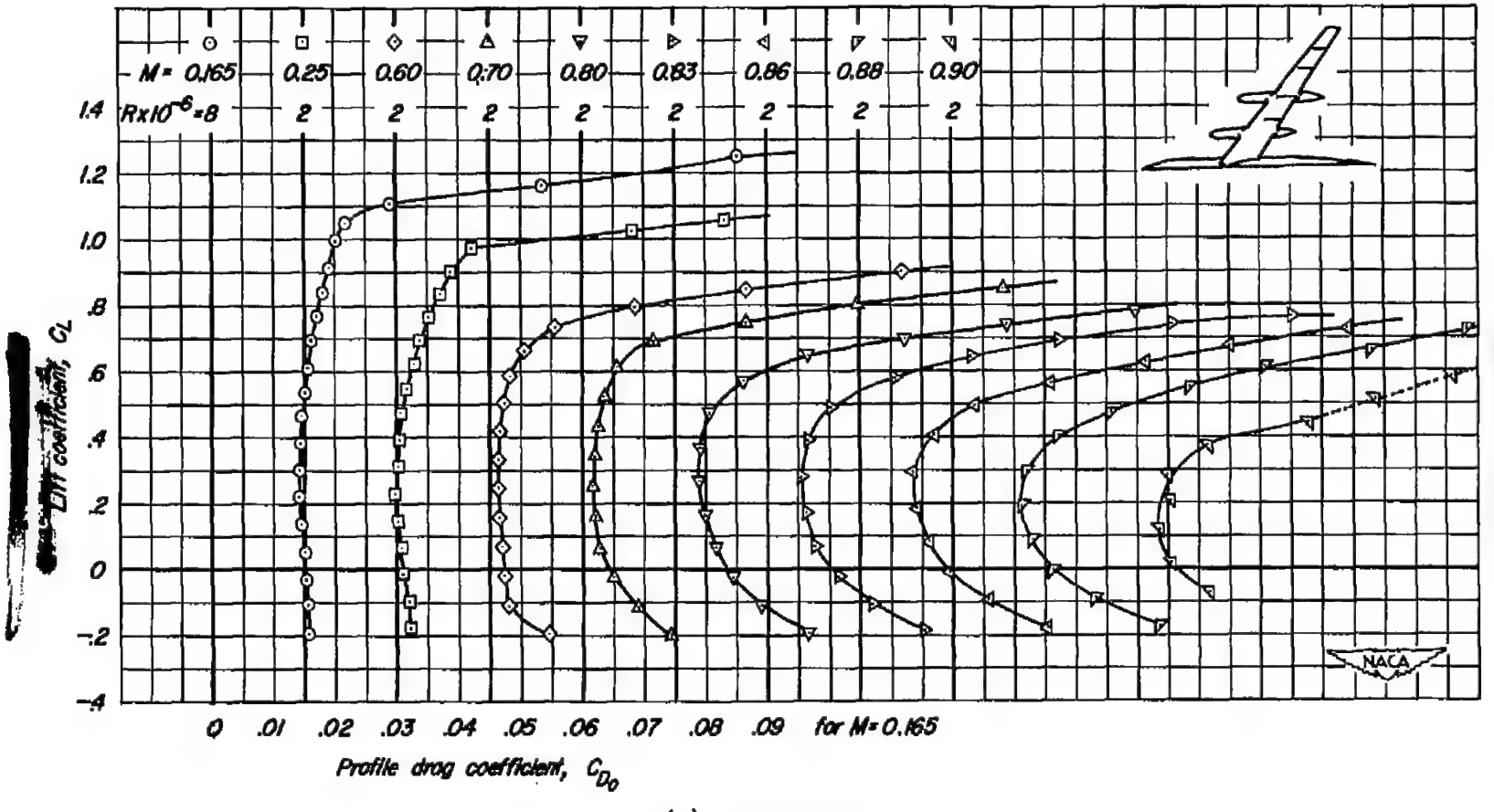

(c) C_{D_o} vs C_L

Figure 3.- Concluded.

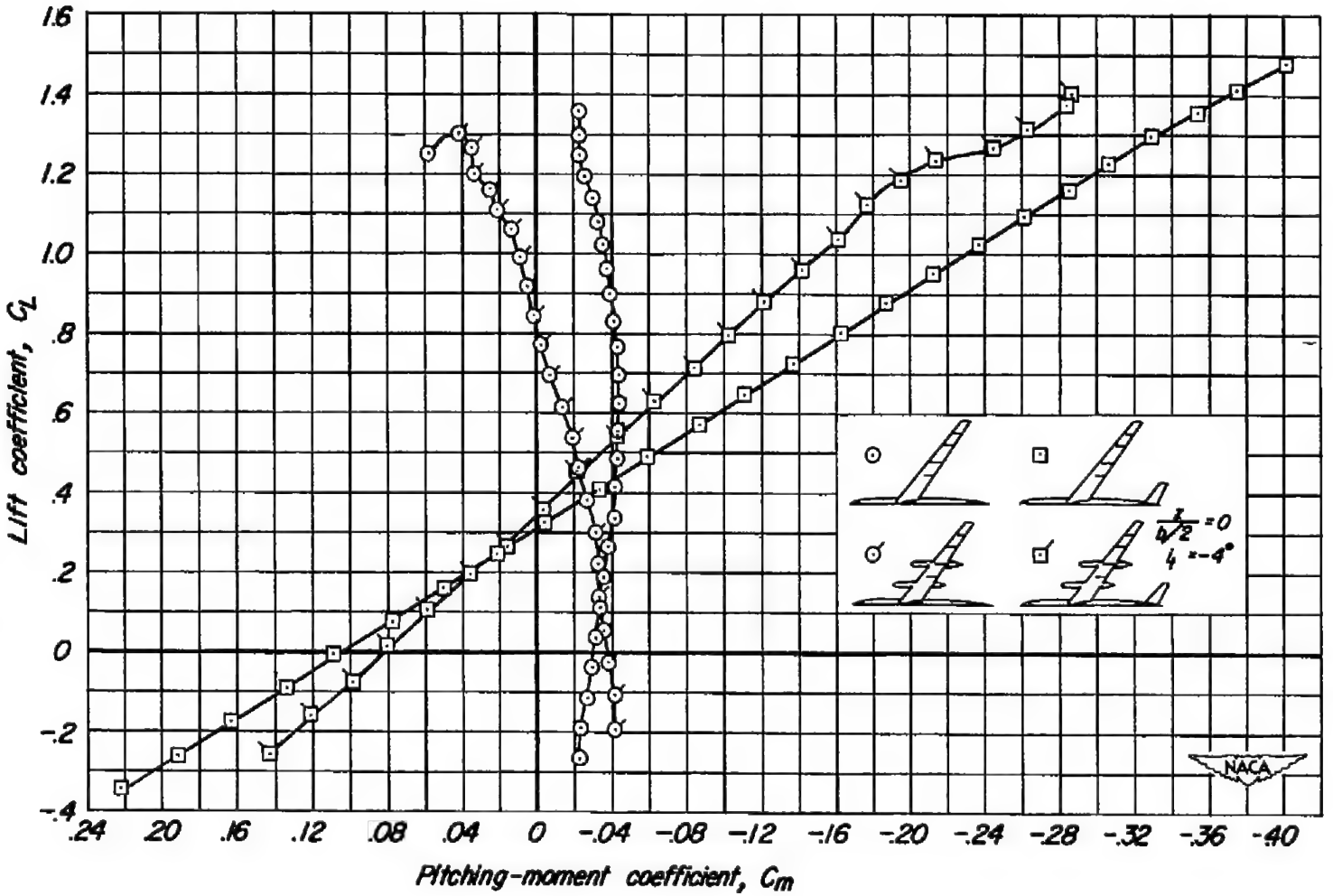

(a) M = 0.165, R = 8,000,000

Figure 4.- The effects of the nacelles on the pitching-moment coefficients.

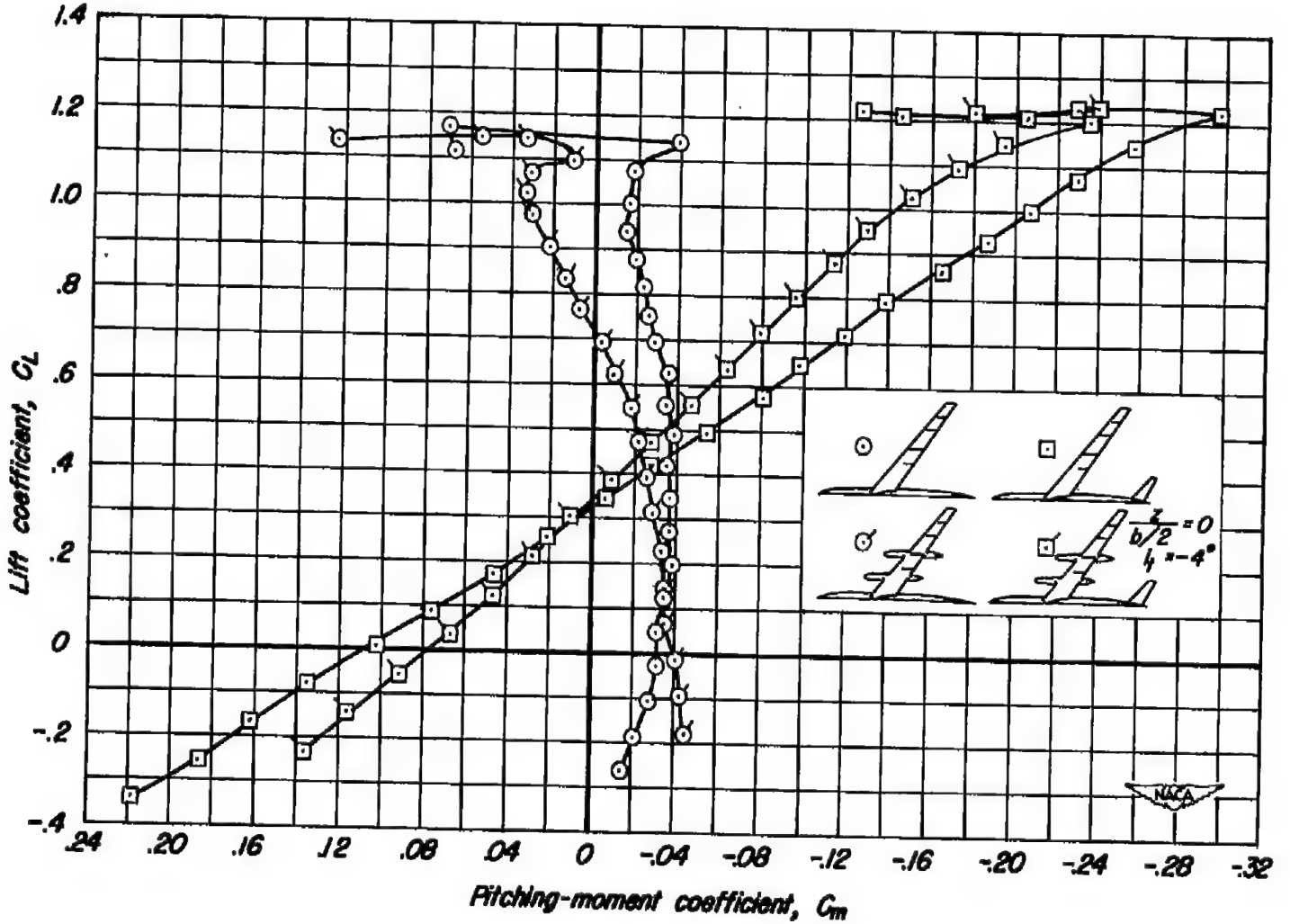

(b) M = 0.25, R = 2,000,000

Figure 4.- Continued.

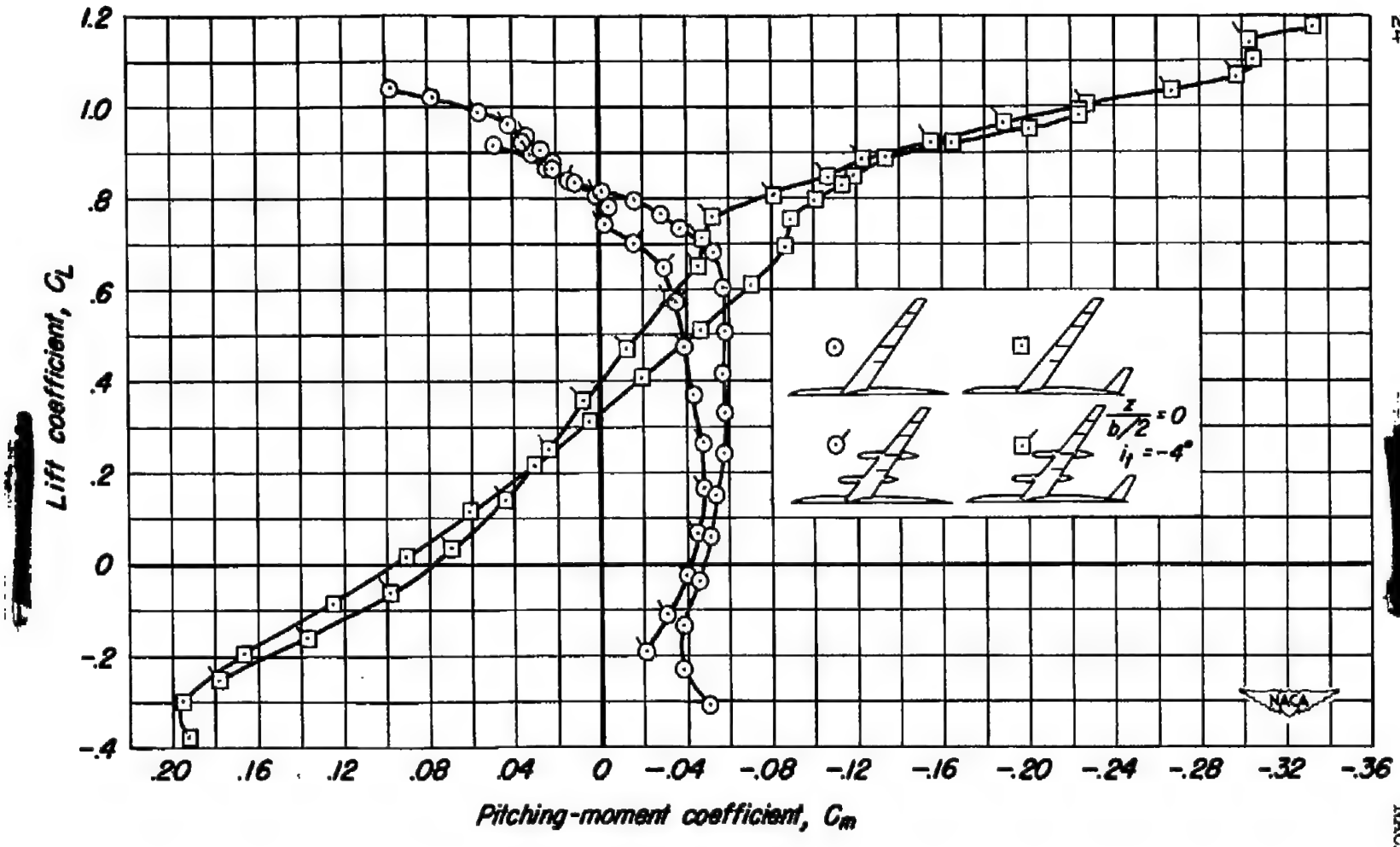

(c) M = 0.80, R = 2,000,000

Figure 4.- Continued.

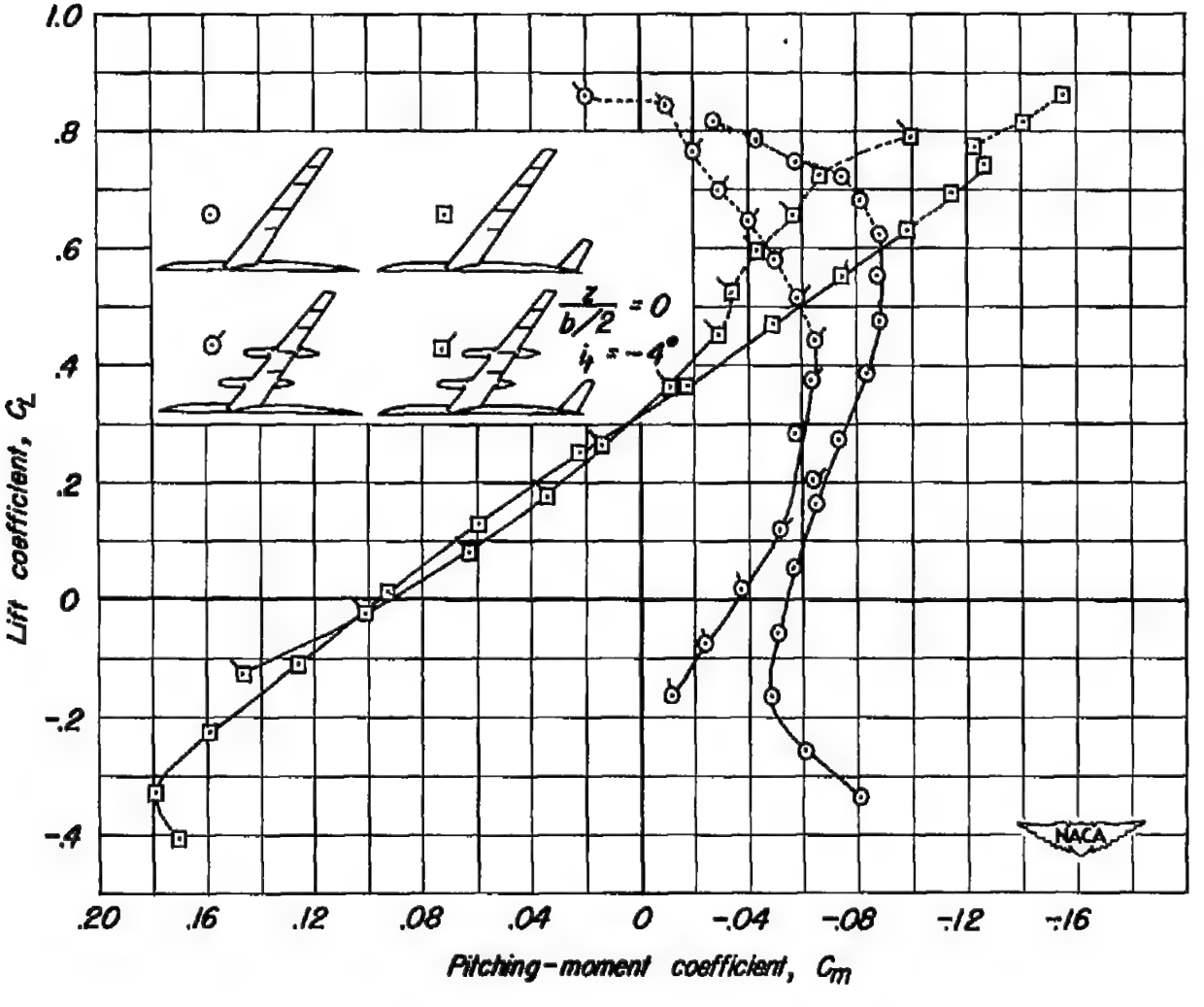

(d) M = 0.90, R = 2,000,000

Figure 4.- Concluded.

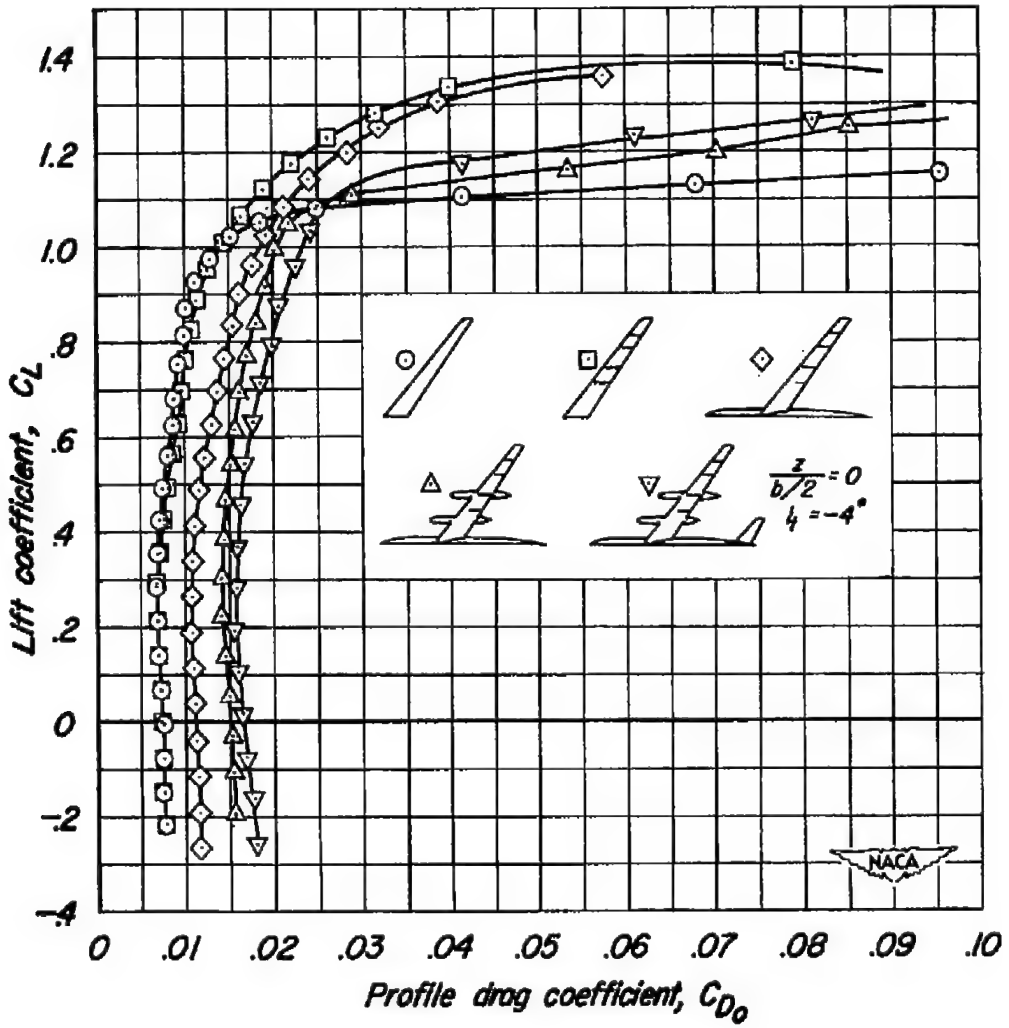

(a) M = 0.165, R = 8,000,000

Figure 5.- The effect on the drag coefficient of the addition of various components to the model.

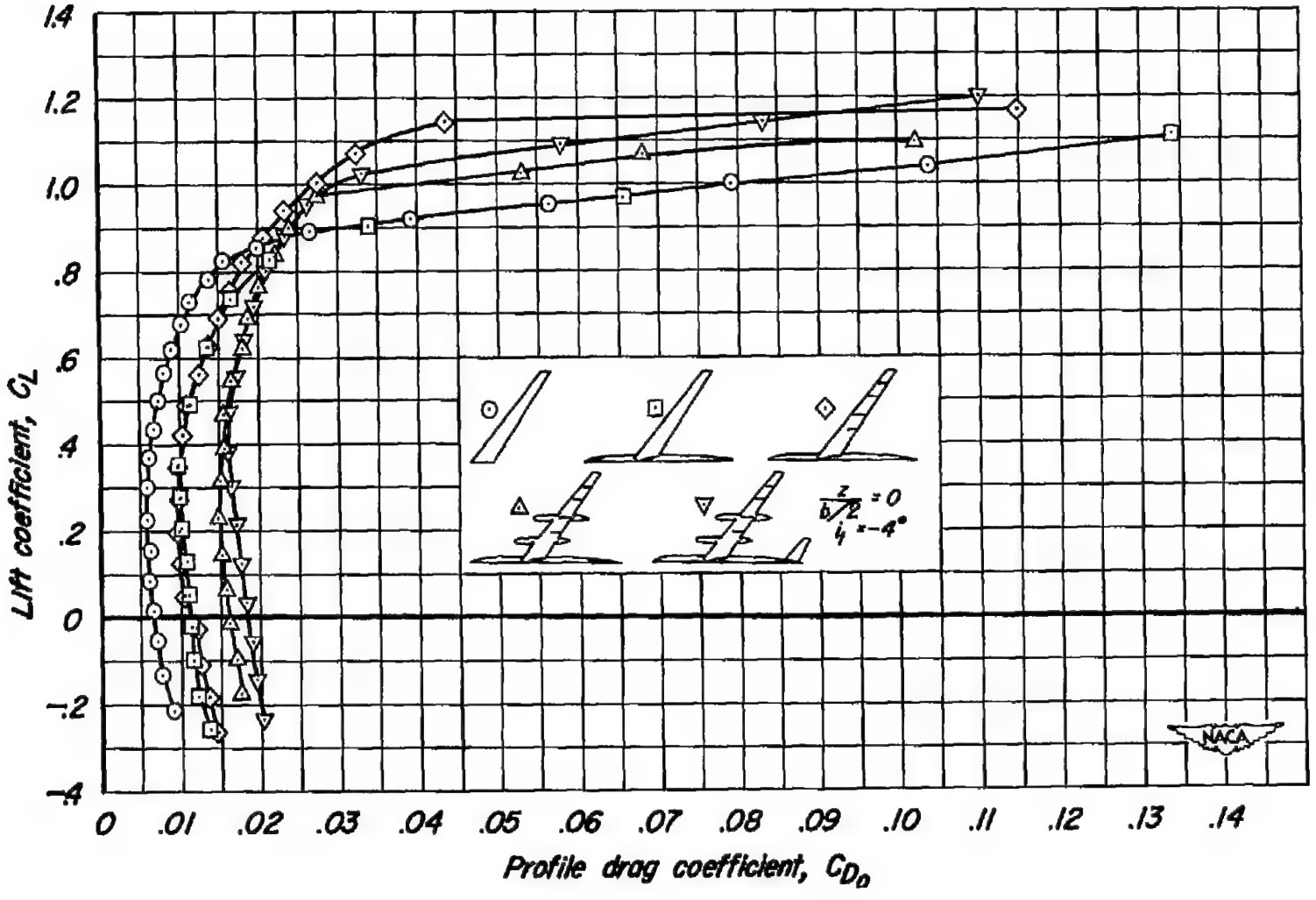

(b) M = 0.25, R = 2,000,000

Figure 5.- Continued.

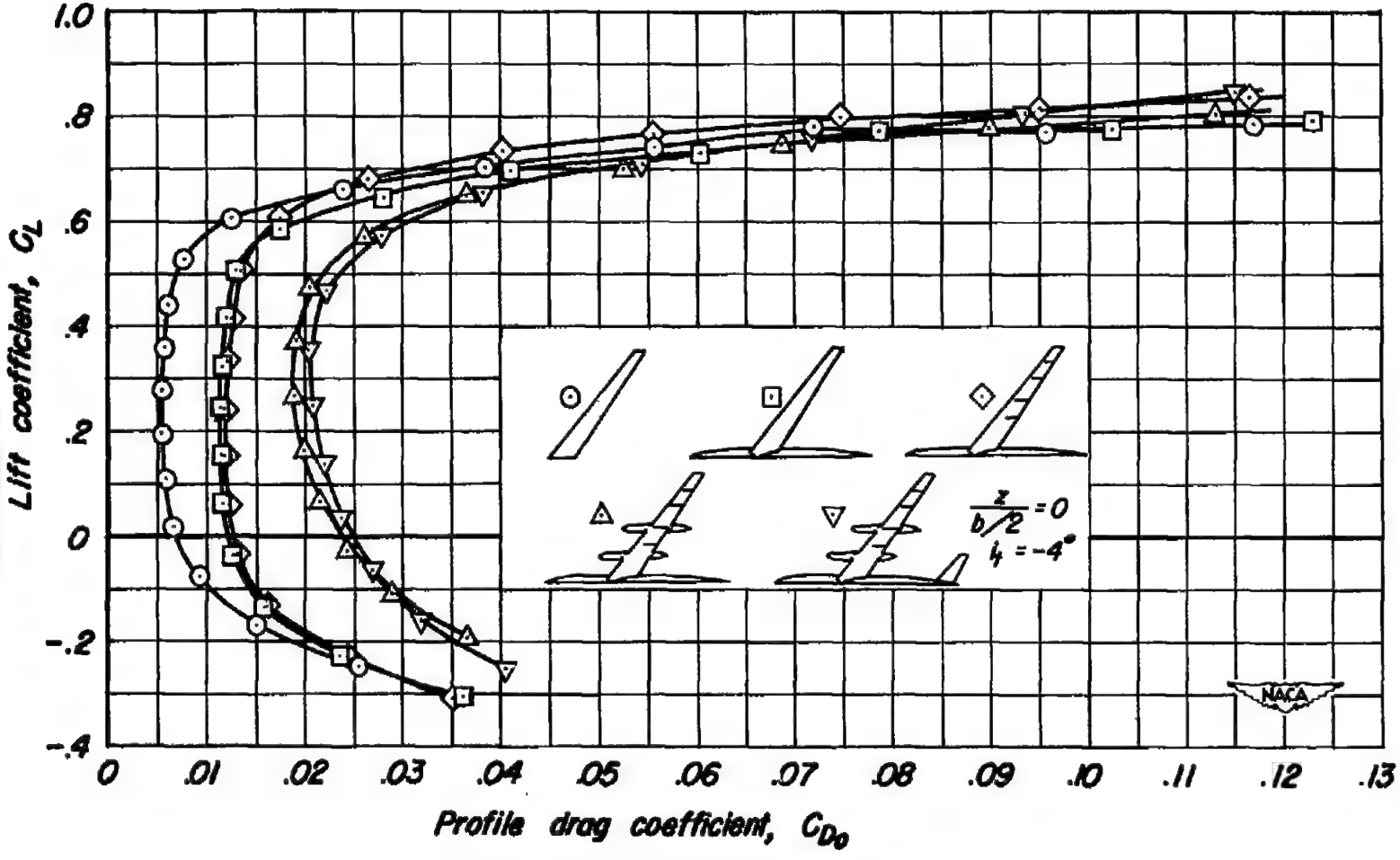

(c) M = 0.80, R = 2,000,000

Figure 5.- Continued.

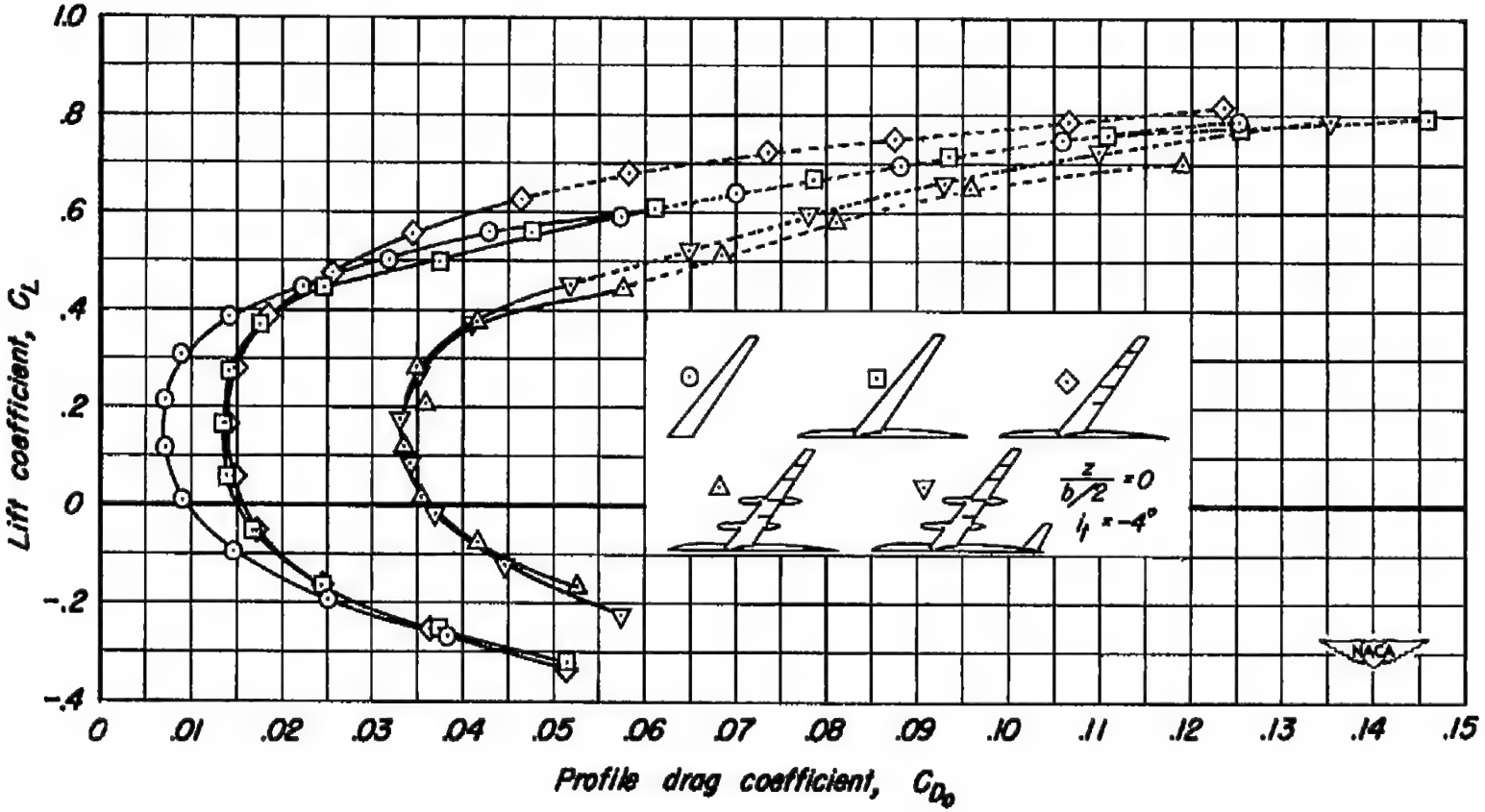

(d) M = 0.90, R = 2,000,000

Figure 5.- Concluded.

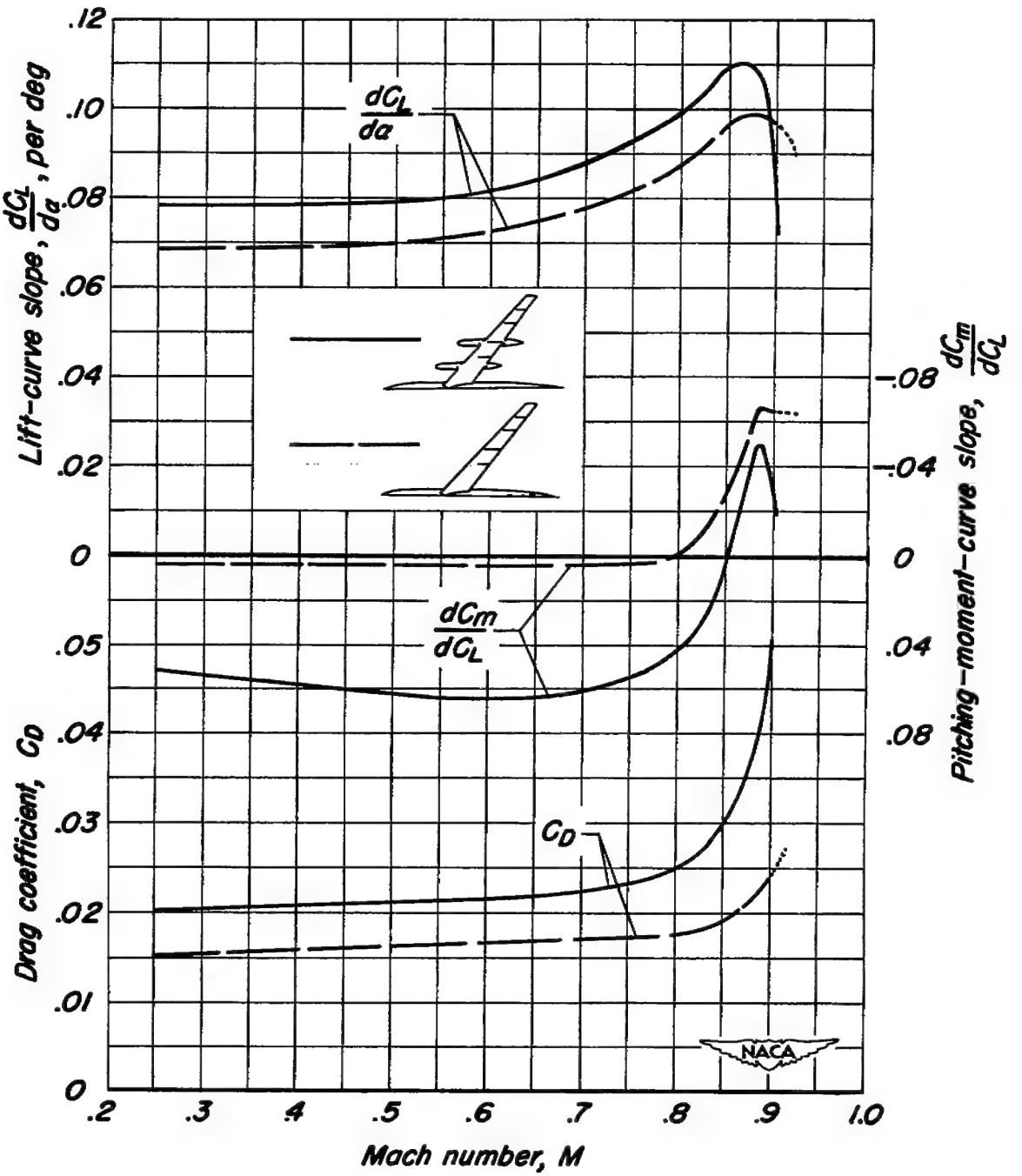

Figure 6.- The effect of the nacelles on the variation with Mach number of the lift-curve slope, the pitching-moment-curve slope, and the drag coefficient. $C_L = 0.4$, R = 2,000,000.

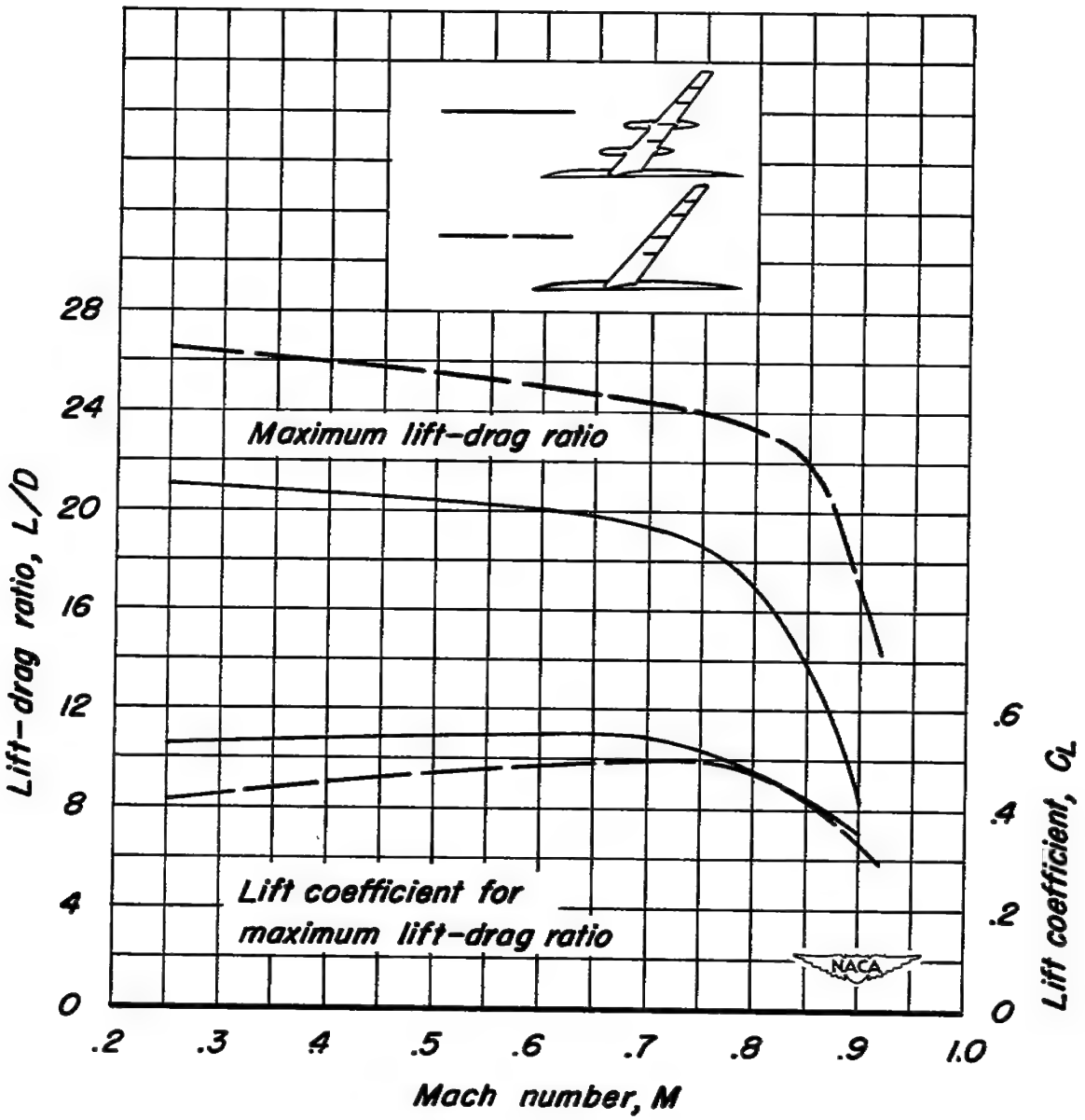

Figure 7.- The effect of nacelles on the variation of maximum lift-drag ratio and of lift coefficient for maximum lift-drag ratio with Mach number. R = 2,000,000.

[redacted]

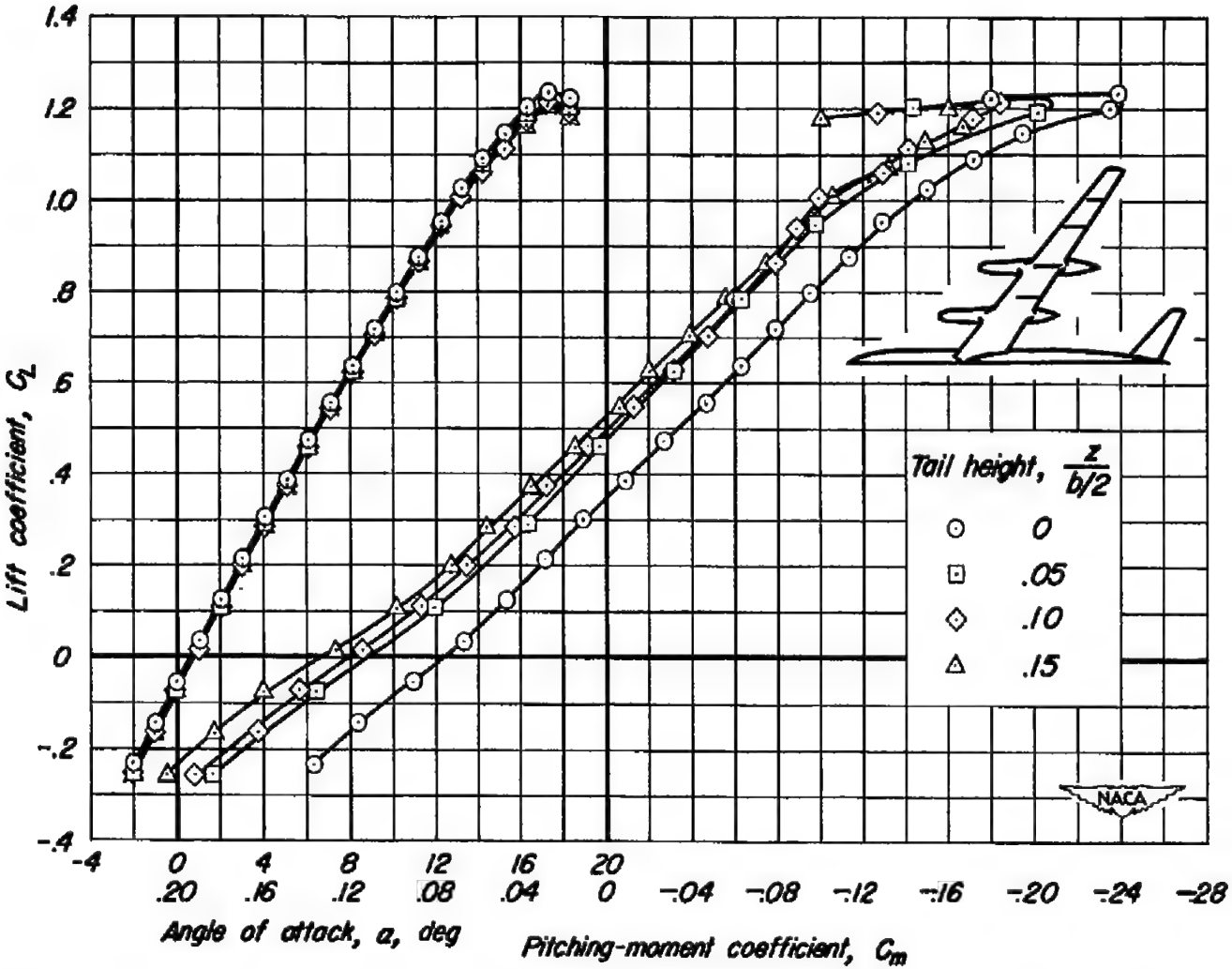

(a) M = 0.25, R = 2,000,000

Figure 8.- The effect of horizontal tail height on the lift and pitching-moment coefficients. $i_t = -4^\circ$.

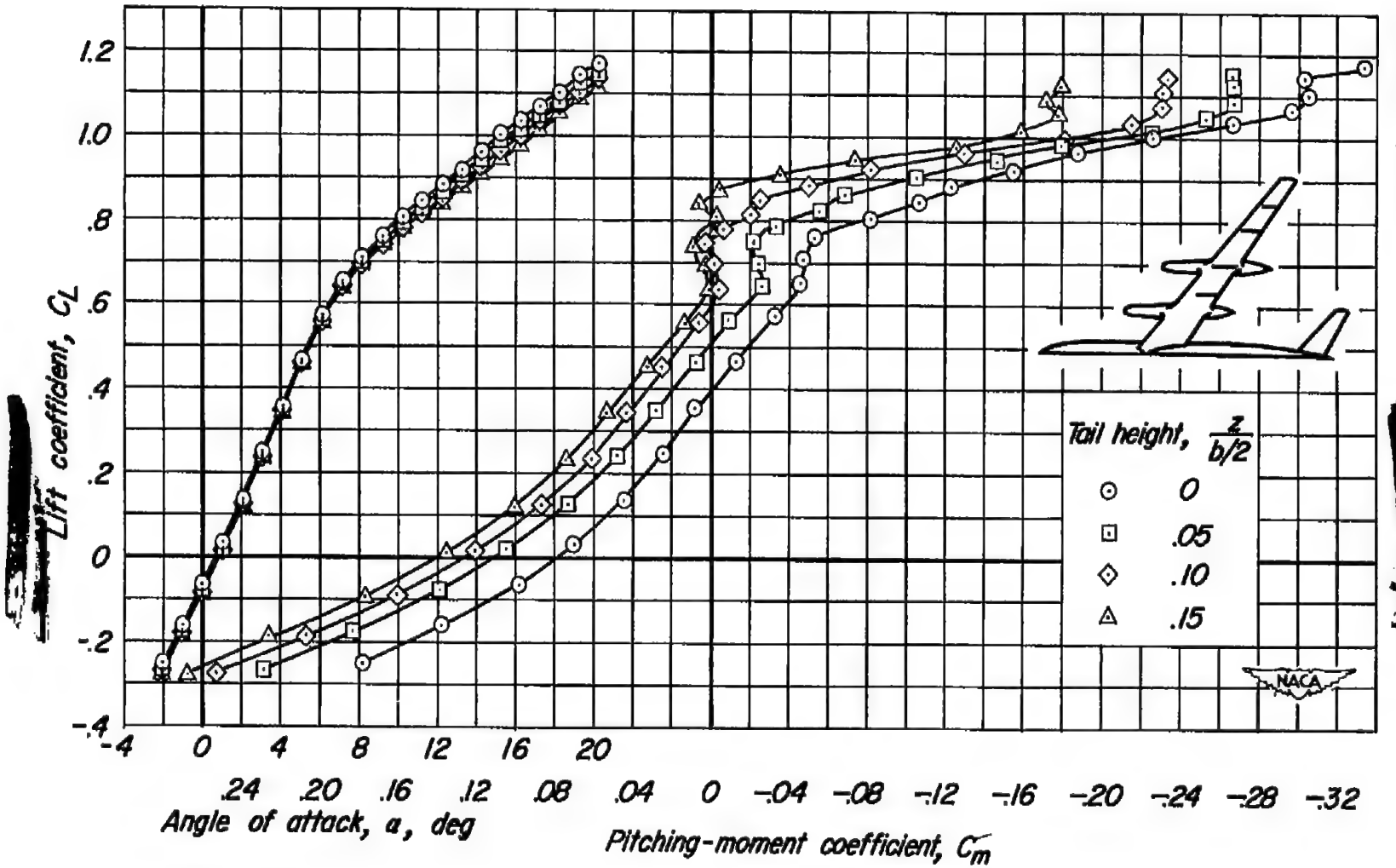

(b) M = 0.80, R = 2,000,000

Figure 8.- Continued.

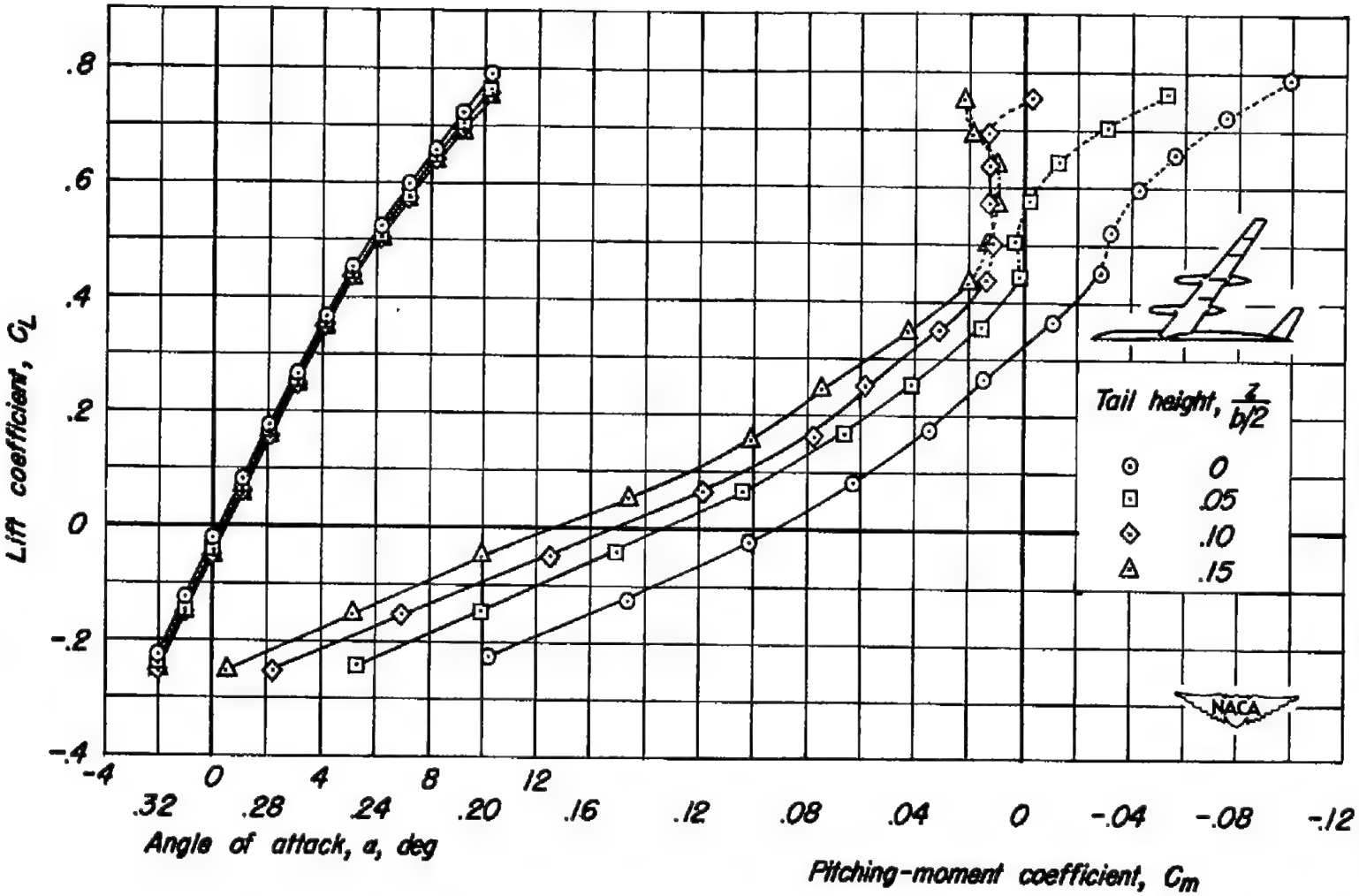

(c) M = 0.90, R = 2,000,000

Figure 8.- Concluded.

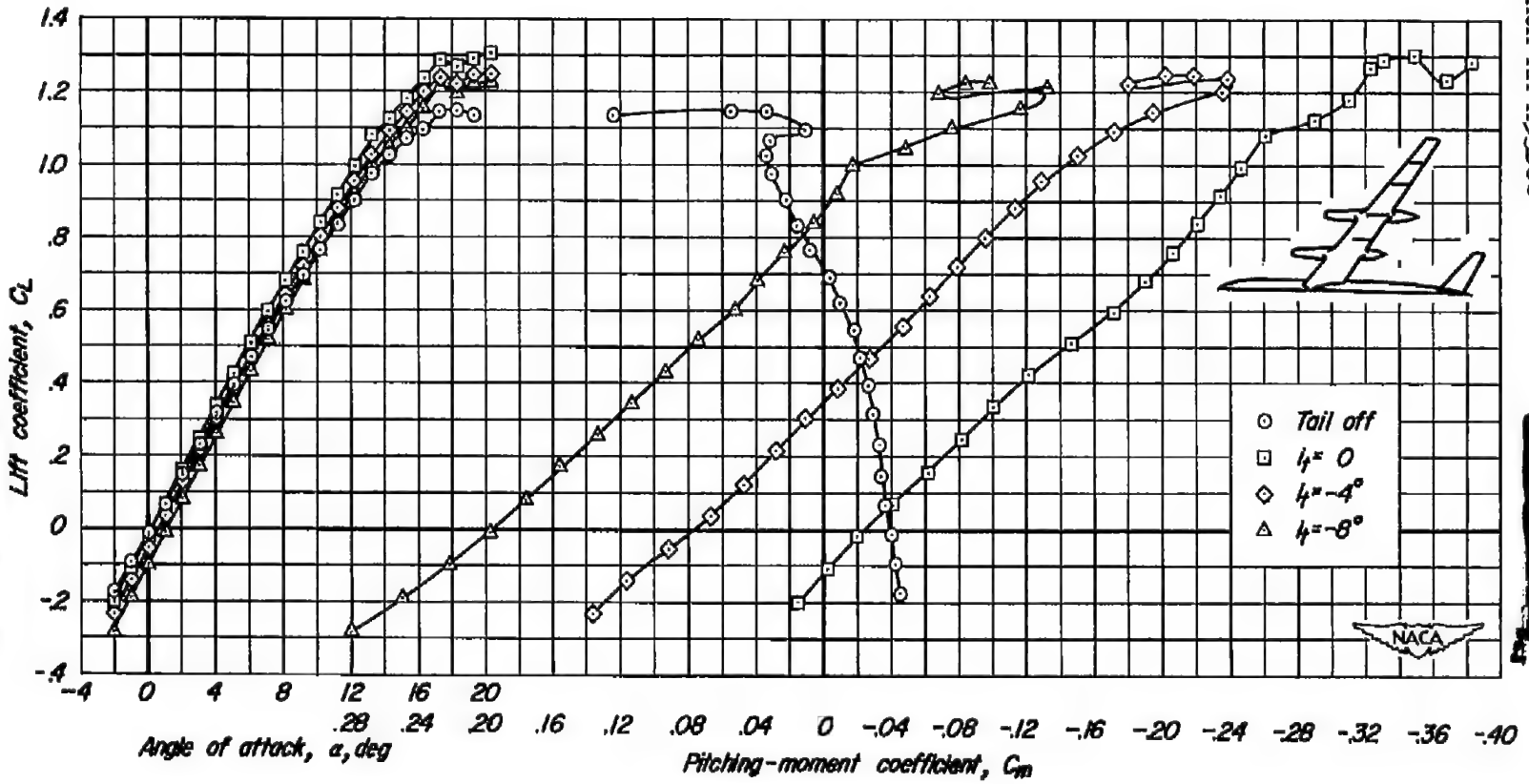

(a) M = 0.25, R = 2,000,000

Figure 9.- The effect of the horizontal tail on the lift and pitching-moment coefficients.

$\frac{z}{b/2} = 0.$

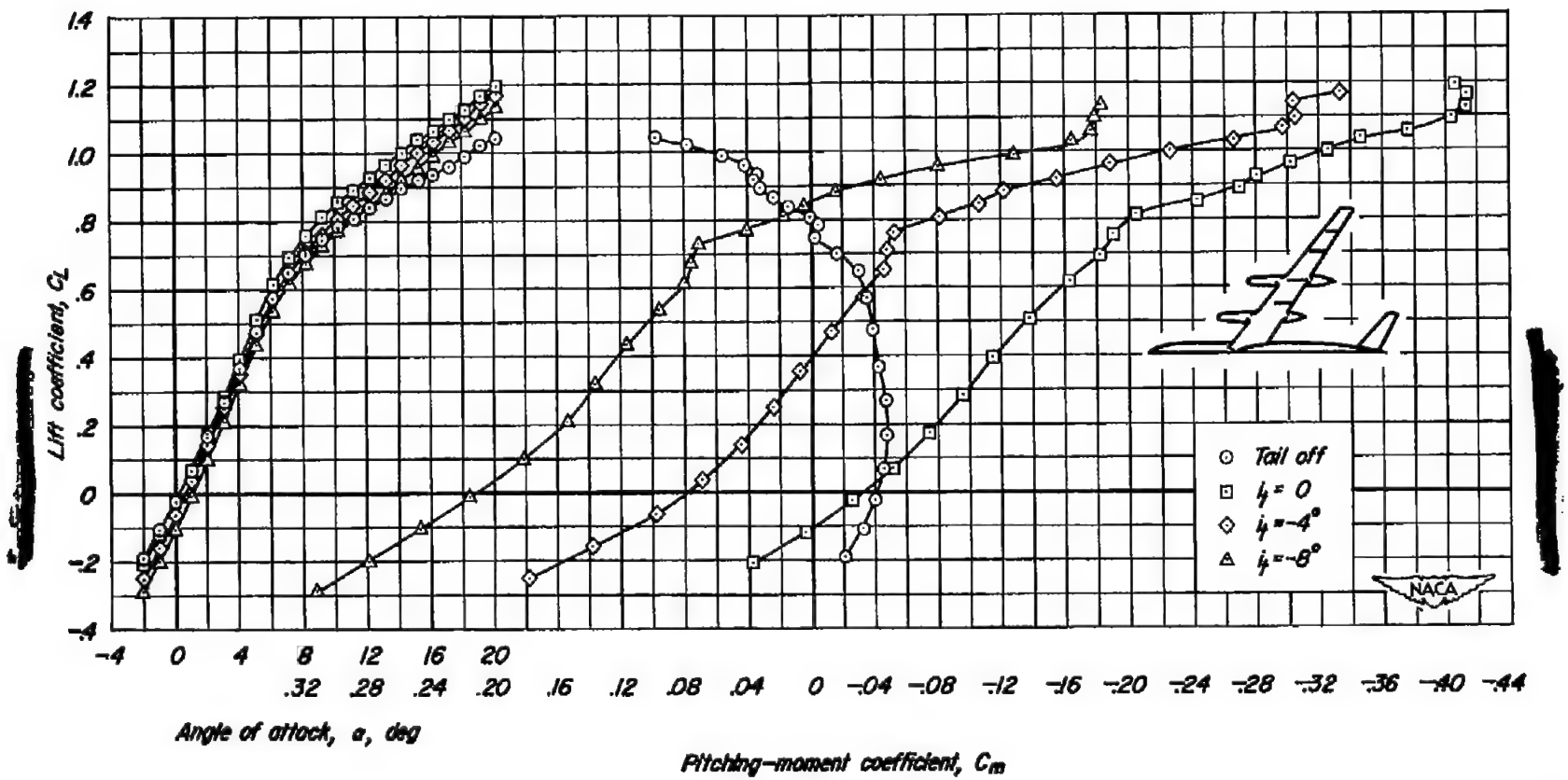

(b) M = 0.80, R = 2,000,000

Figure 9.- Continued.

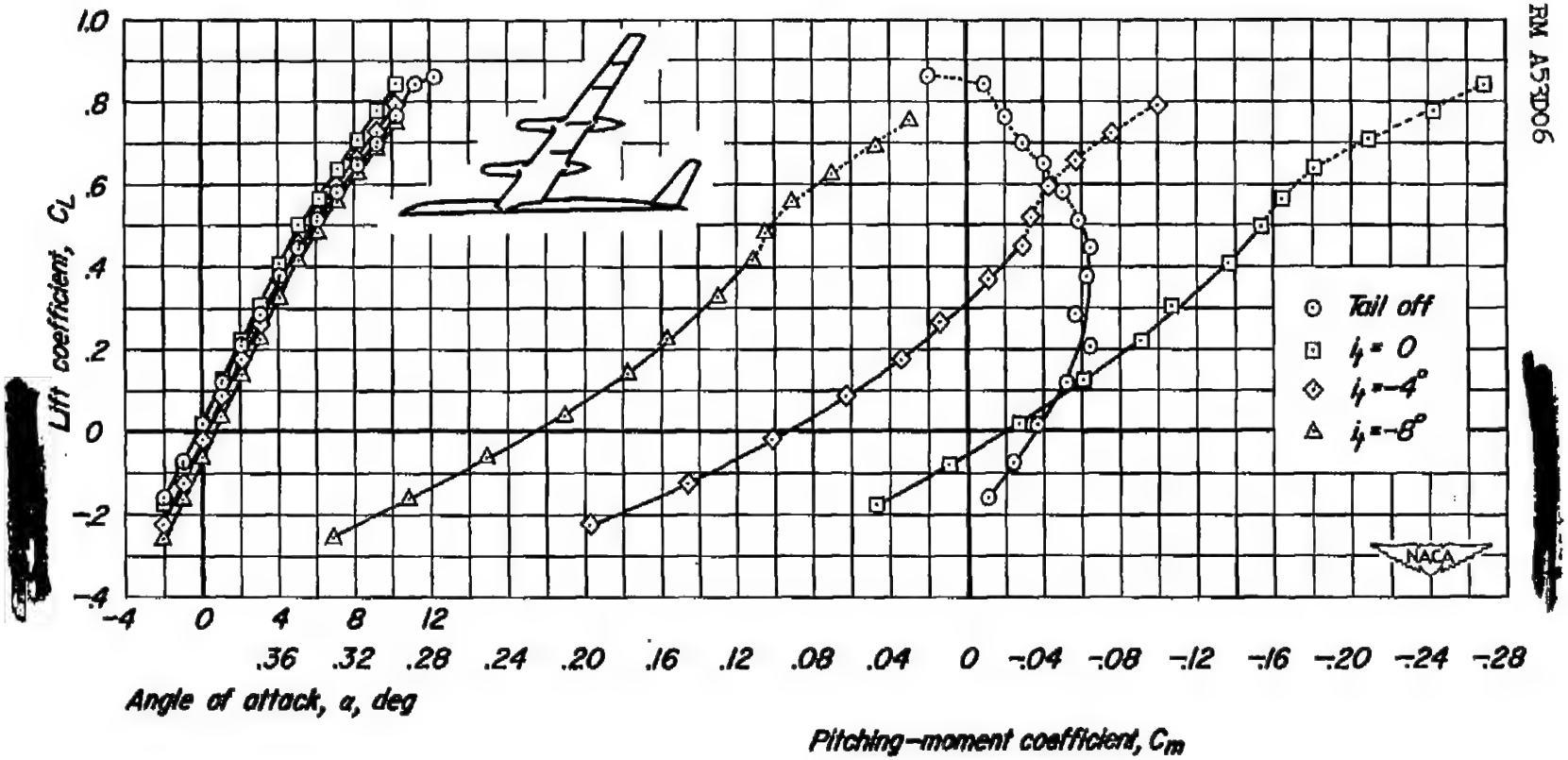

(c) M = 0.90, R = 2,000,000

Figure 9.- Concluded.

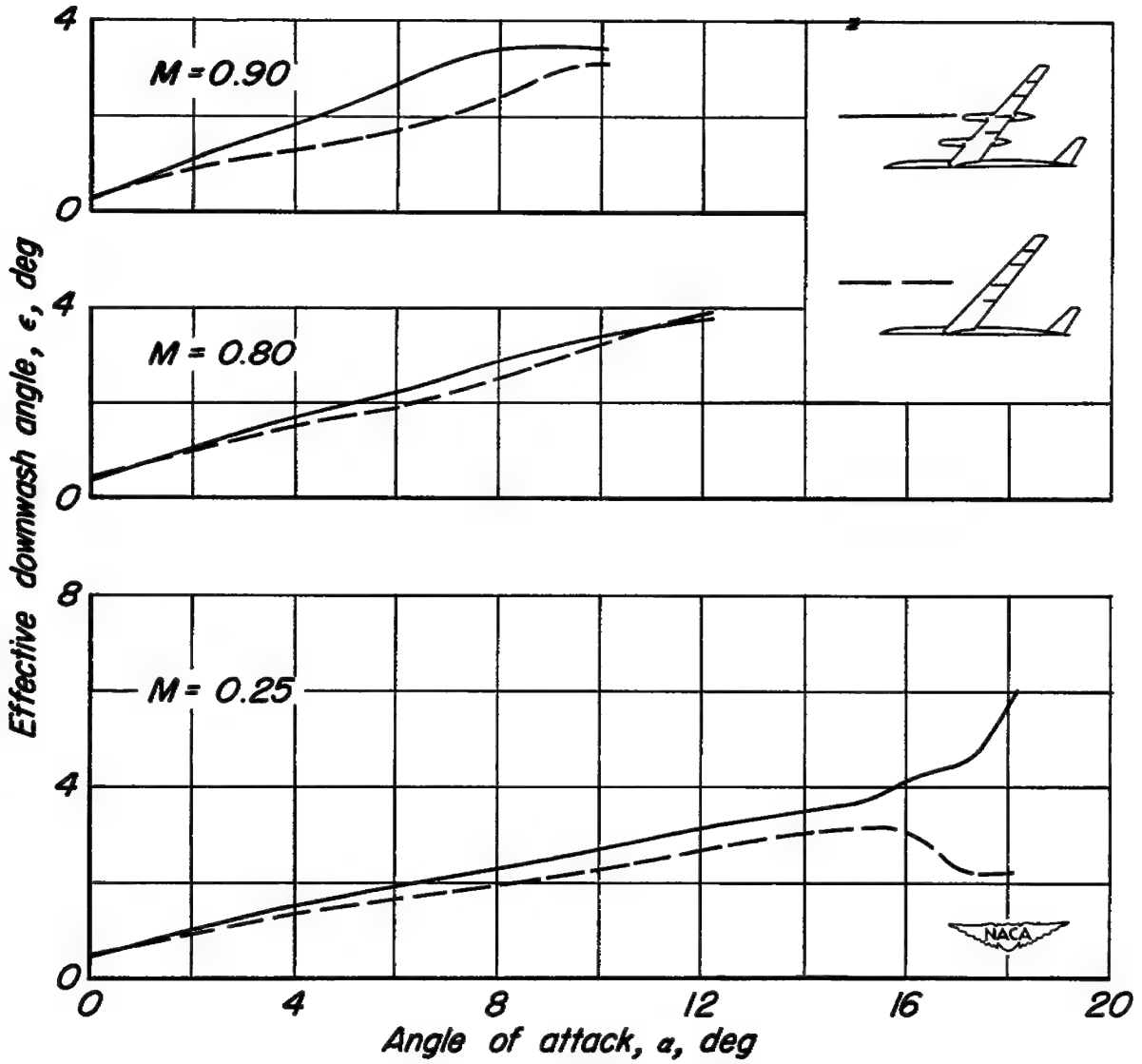

Figure 10.- The effect of the nacelles on the effective downwash angle. $\frac{z}{b/2} = 0$, R = 2,000,000.

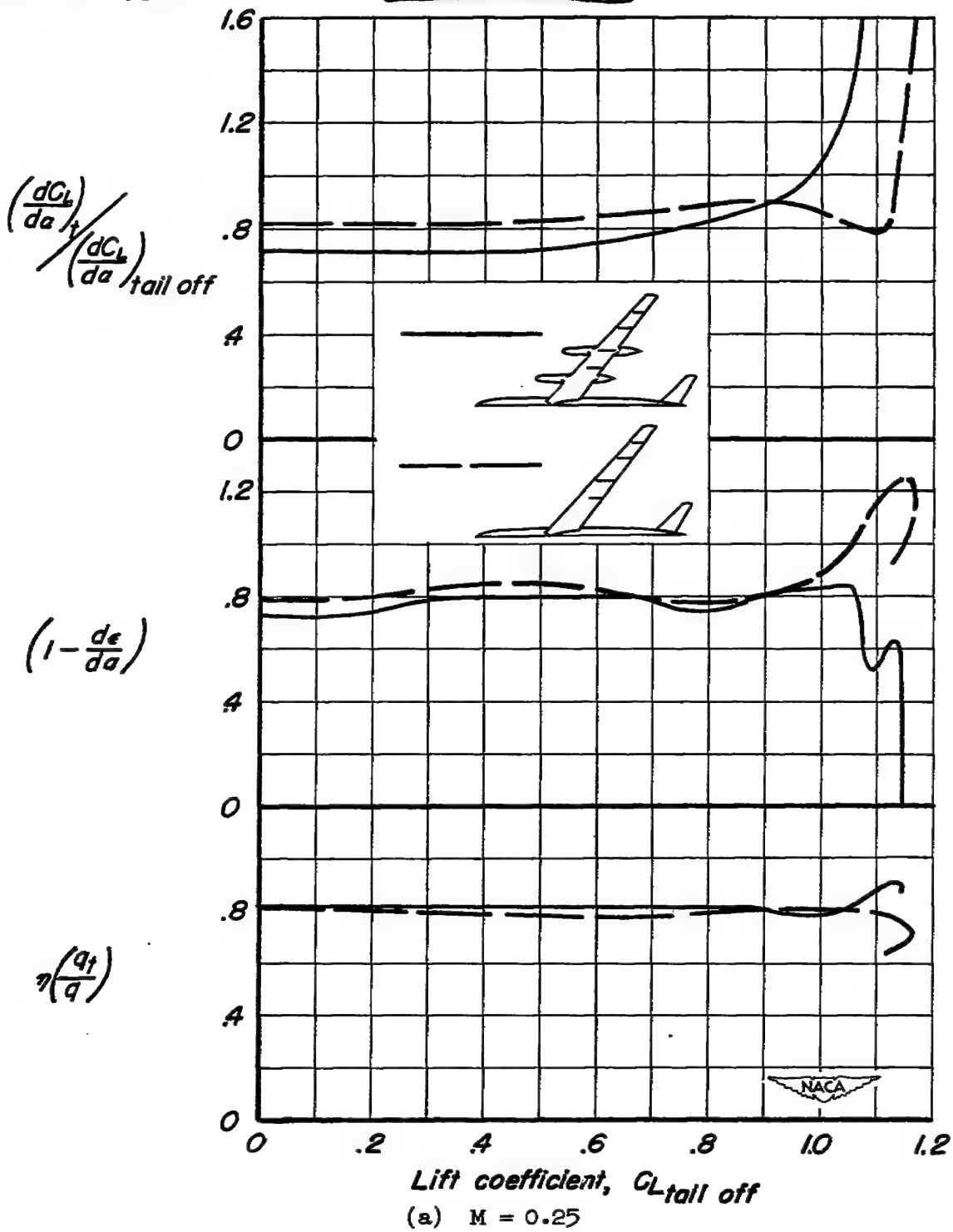

(a) M = 0.25

Figure 11.- The effect of the nacelles on the variation with lift coefficient of the factors affecting the stability contribution of the horizontal tail. R[redacted]

[redacted]

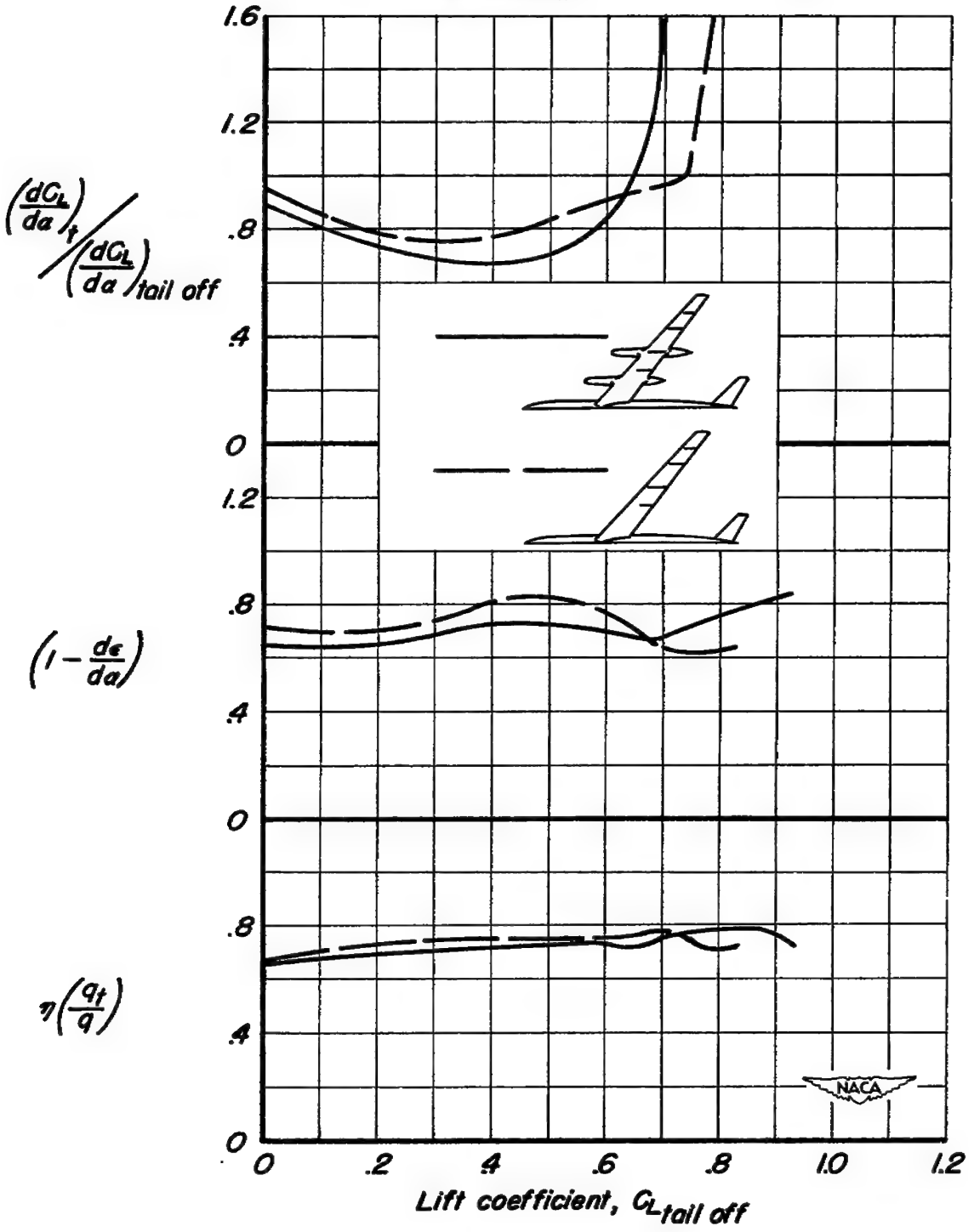

(b) M = 0.80

Figure 11.- Concluded.

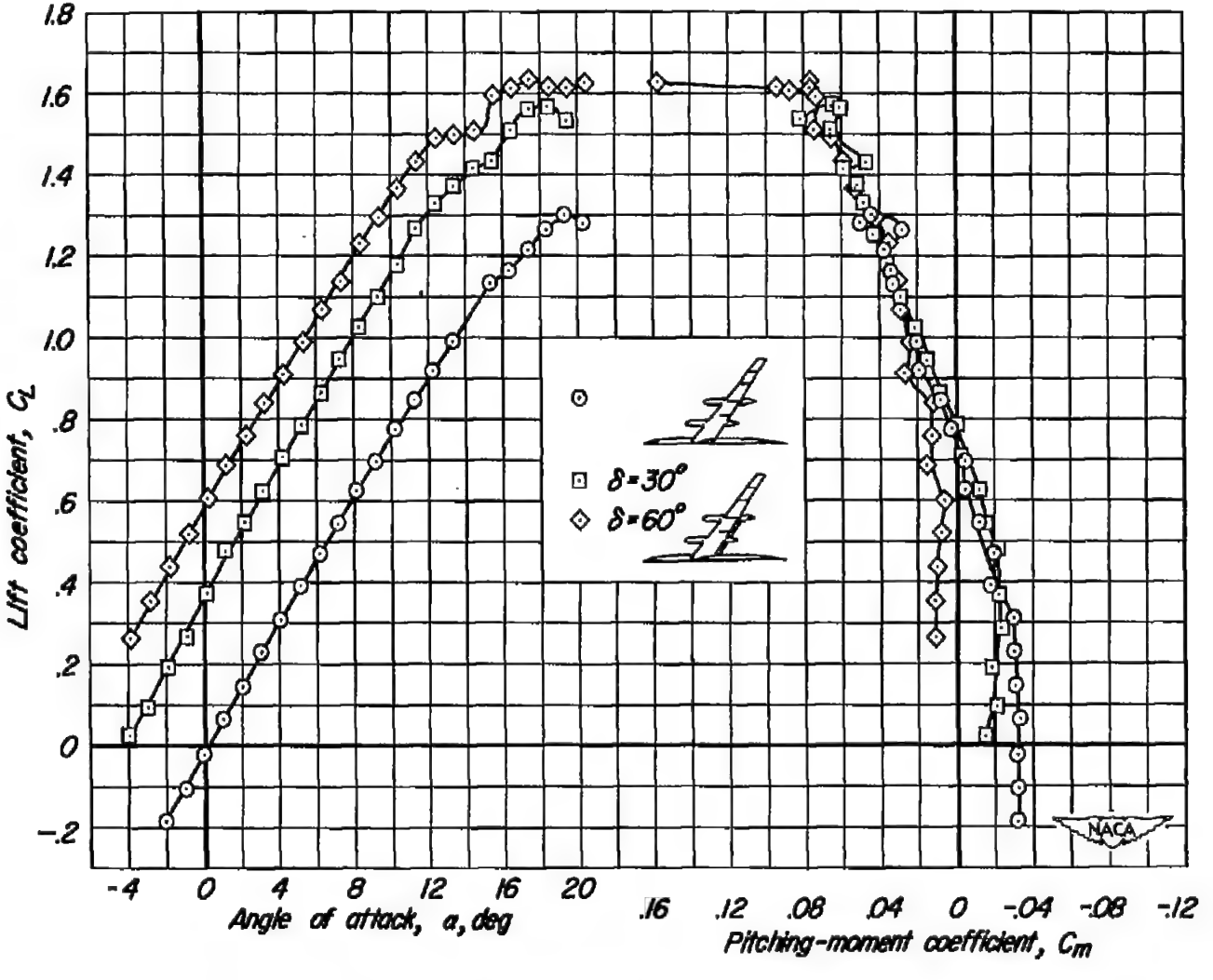

Figure 12.- The effects of flaps on the lift and pitching-moment coefficients. M = 0.082, R = 4,000,000.

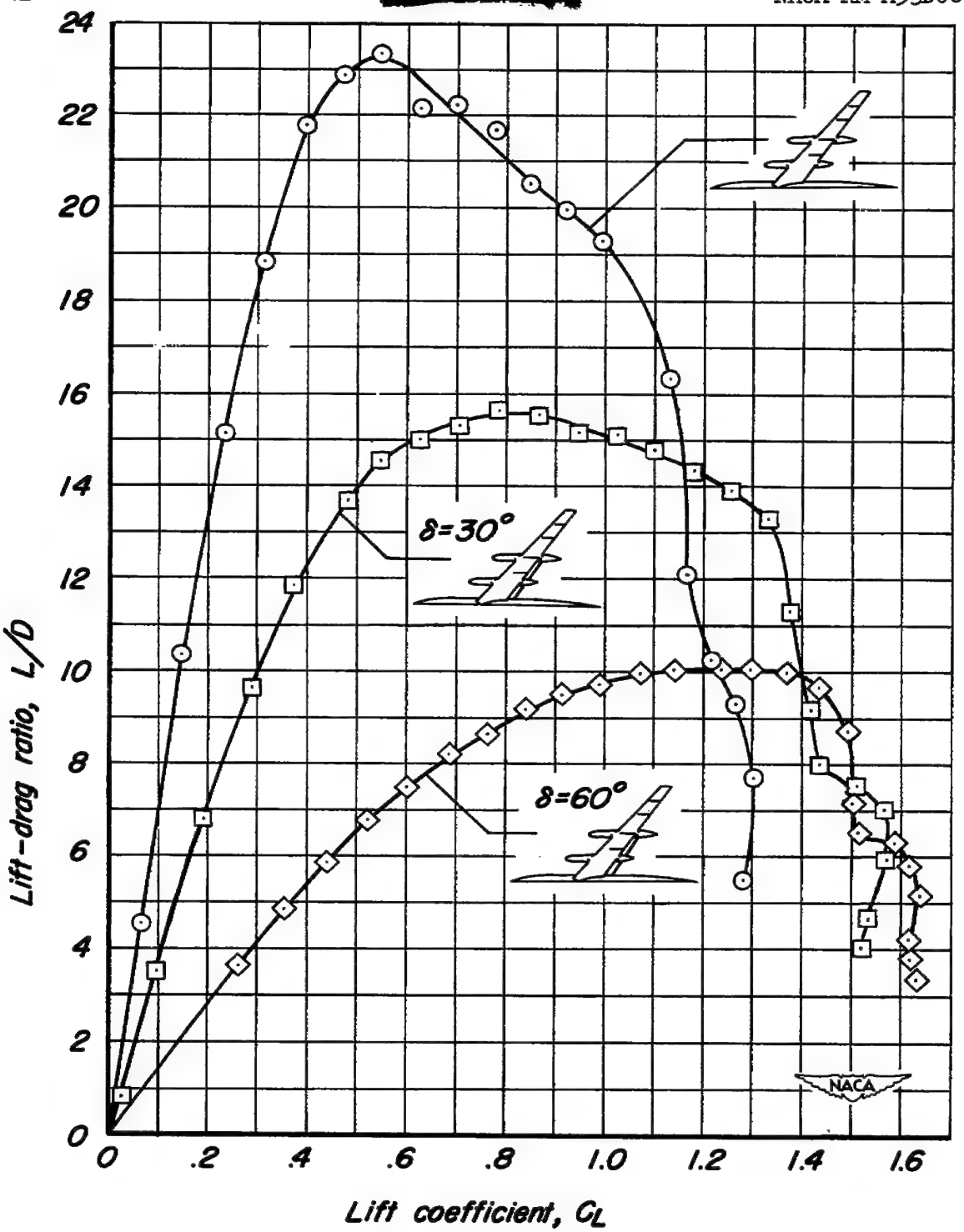

Figure 13.- The effect of flaps on the lift-drag ratio.
M = 0.082, R = 4,000,000.

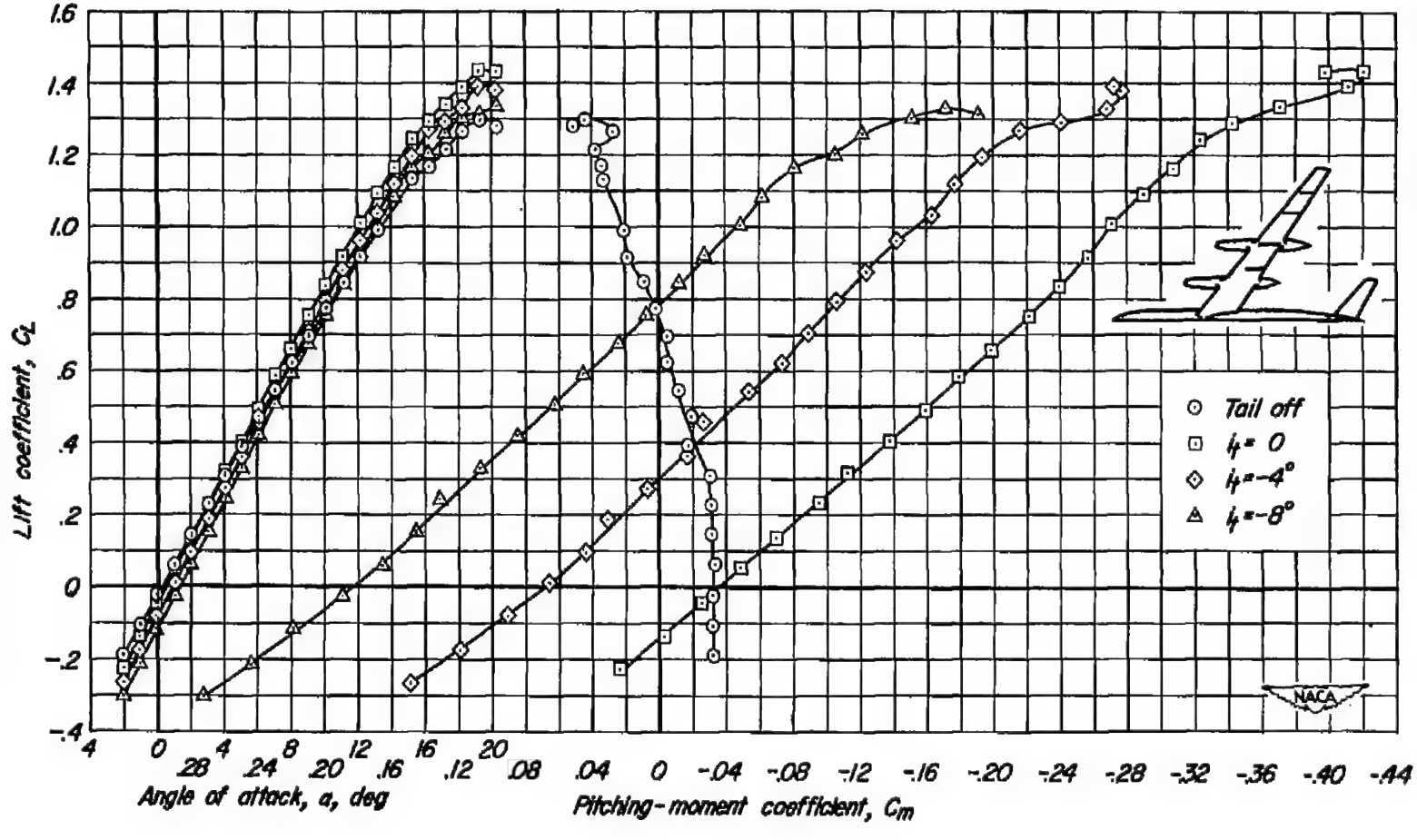

(a) Flaps off.

Figure 14.- The effect of the horizontal tail on the lift and pitching-moment coefficients. M = 0.082, R = 4,000,000, $\frac{z}{b/2} = 0$.

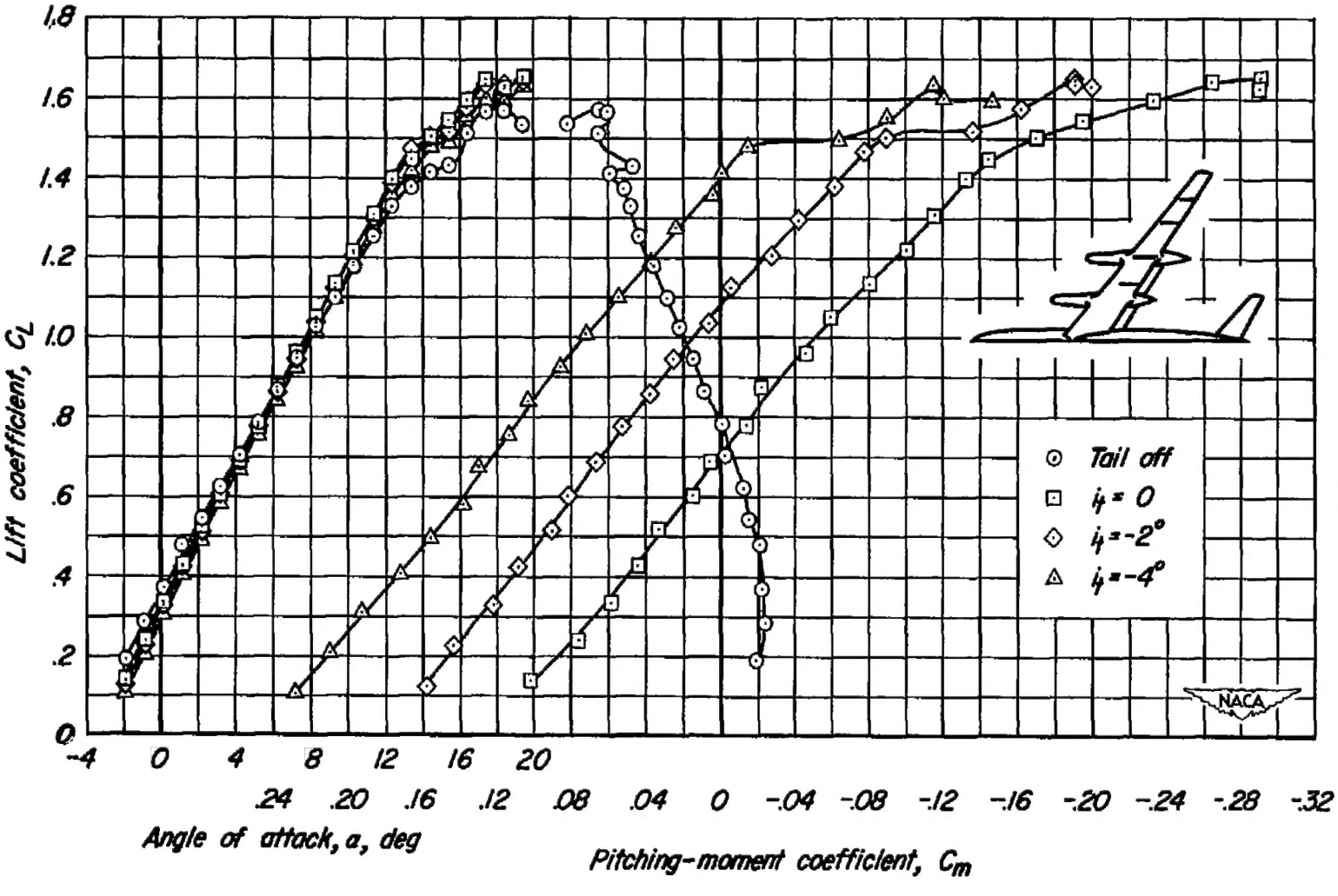

(b) Extended split flaps deflected 30°.

Figure 14.- Concluded.

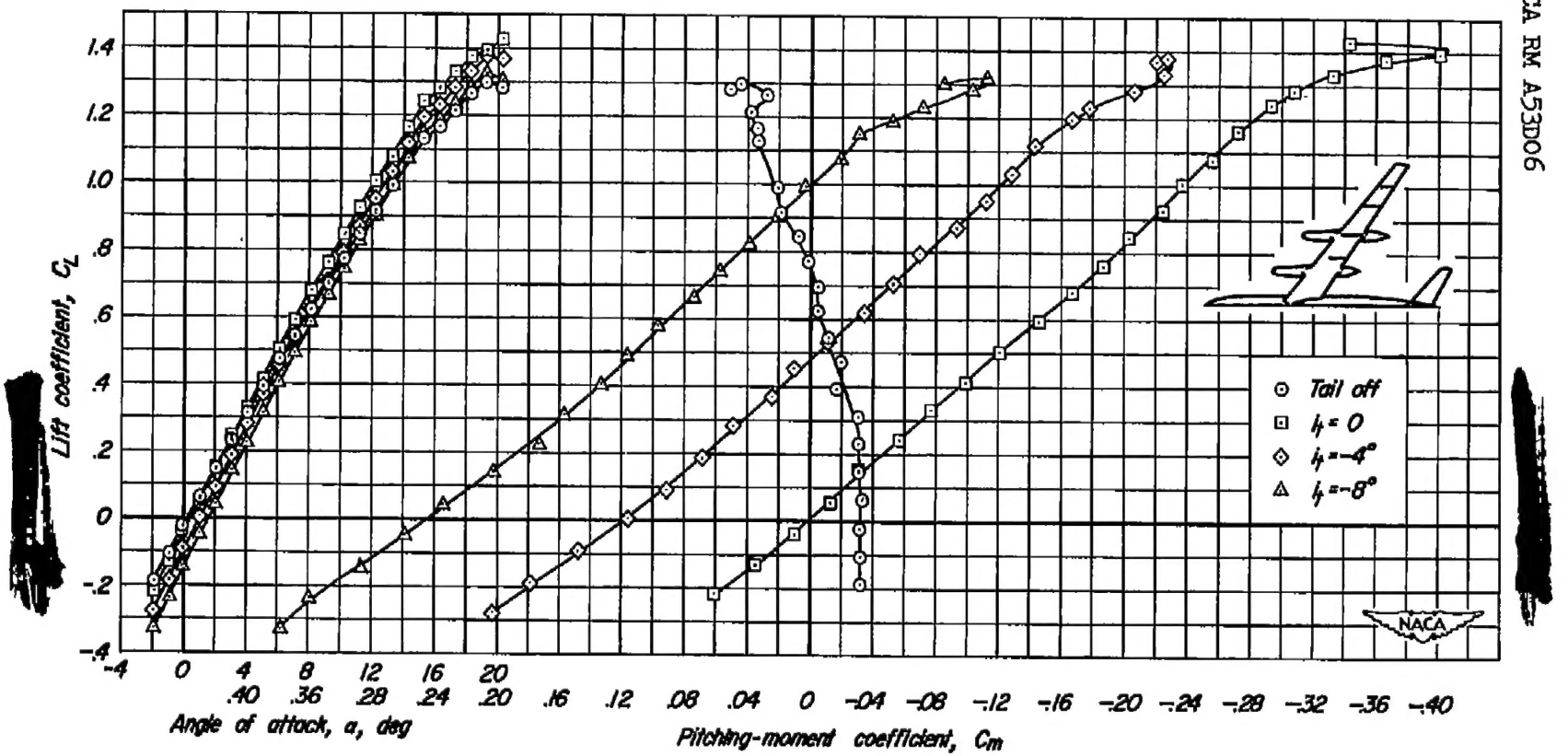

(a) Flaps off.

Figure 15.- The effect of the horizontal tail on the lift and pitching-moment coefficients. $M = 0.082$, $R = 4{,}000{,}000$, $\frac{z}{b/2} = 0.10$.

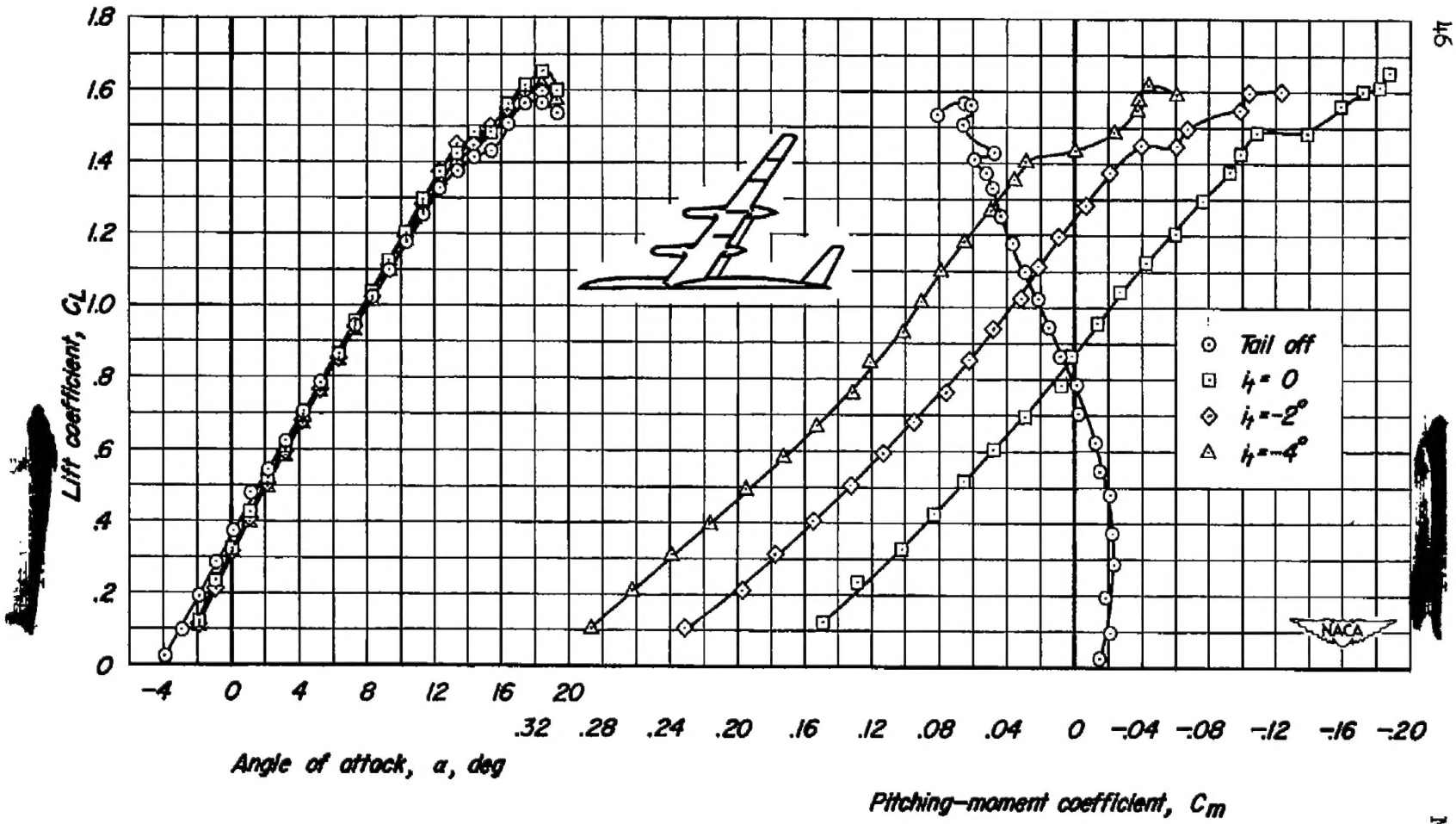

(b) Extended split flaps deflected 30°.

Figure 15.- Concluded.

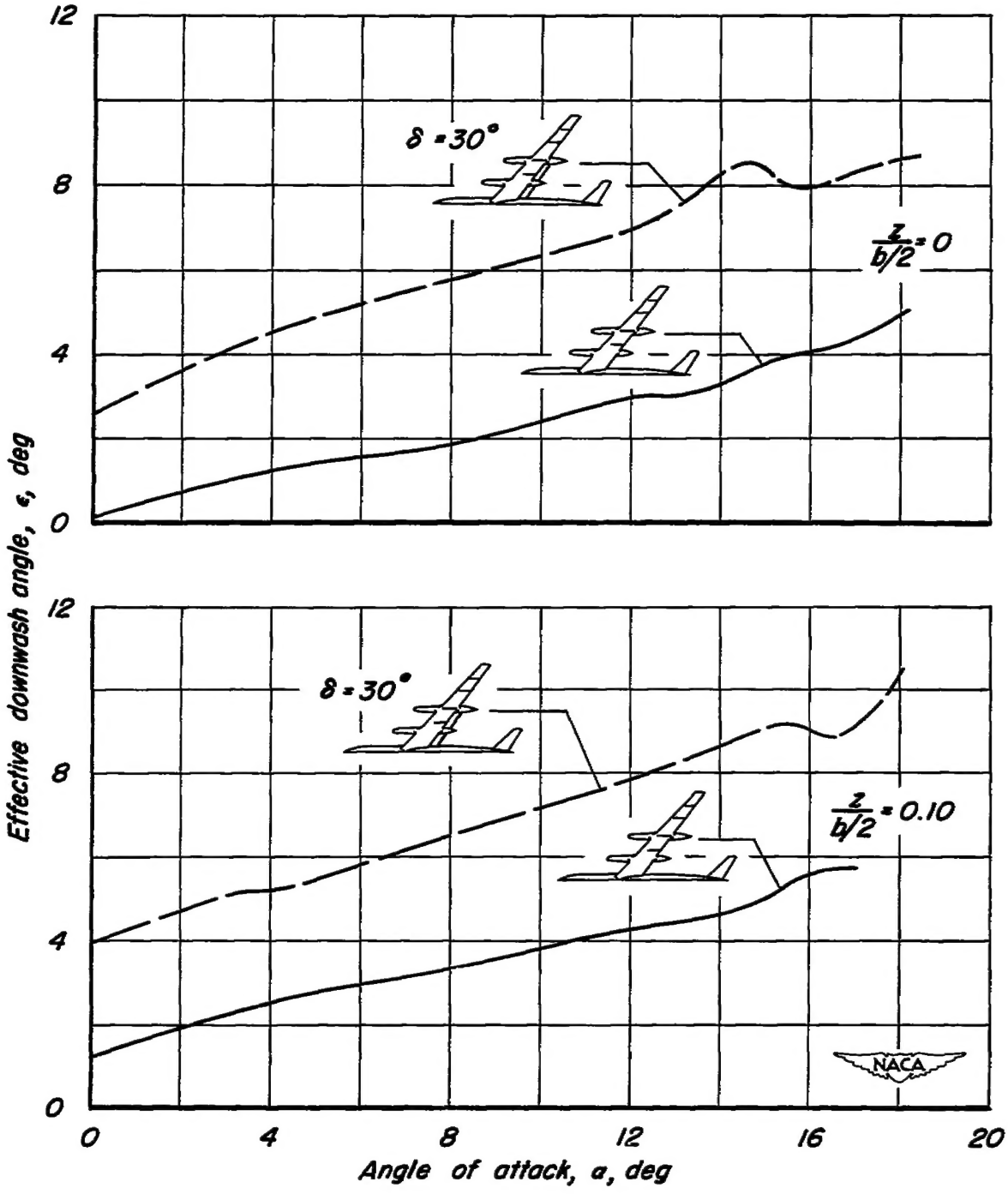

Figure 16.- The effect of the flaps on the effective downwash angle for two tail heights. M = 0.082, R = 4,000,000.

[redacted]